

# Rectified-CFG++ for Flow Based Models

Anonymous Author(s)

Affiliation

Address

email

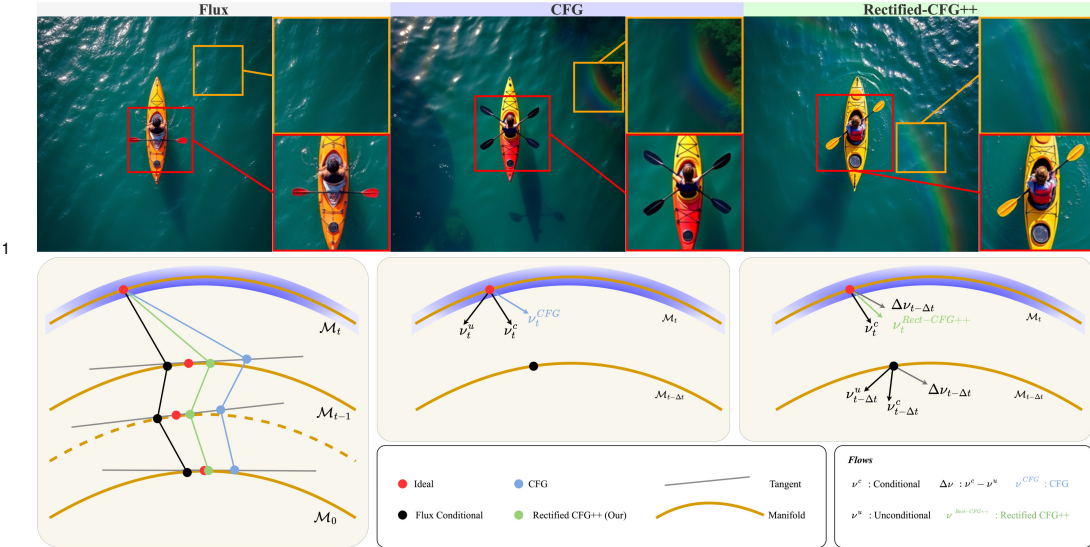


Figure 1: **Top:** Visual outputs from Flux, w/ standard CFG, and w/ Rectified-CFG++ for **Prompt: Kayak in the water; optical color; aerial view; rainbow**. While CFG amplifies detail, it introduces artifacts such as oversaturation and structural distortion. Rectified-CFG++ produces semantically faithful results with improved alignment and texture realism. **Bottom:** A conceptual manifold view of sampling dynamics. (*Left*) Conditional and unconditional flows diverge across latent manifolds  $\mathcal{M}_t$ . (*Middle*) CFG combines them by *extrapolation*, forcing the trajectory outside  $\mathcal{M}_t$  (blue path). (*Right*) Rectified-CFG++ first steps along the conditional field then applies a scheduled interpolation towards the unconditional field, keeping the iterate inside the manifold family (green path) and thus avoiding artifacts while improving prompt alignment.

## Abstract

Classifier-free guidance (CFG) is the workhorse for steering large diffusion models toward text-conditioned targets, yet its naïve application to rectified flow (RF) based models provokes severe off-manifold drift, yielding visual artifacts, text misalignment, and brittle behaviour. We present Rectified-CFG++, an adaptive predictor–corrector guidance that couples the deterministic efficiency of rectified flows with a geometry-aware conditioning rule. Each inference step first executes a conditional RF update that anchors the sample near the learned transport path, then applies a weighted conditional correction that interpolates between conditional and unconditional velocity fields. We prove that the resulting velocity field is marginally consistent and that its trajectories remain within a bounded tubular neighbourhood of the data manifold, ensuring stability across a wide range of guidance strengths. Extensive experiments on large-scale text-to-image models (Flux, Stable Diffusion 3/3.5, Lumina) show that Rectified-CFG++ consistently outperforms standard CFG on benchmark datasets such as MS-COCO, LAION-Aesthetic, and T2I-CompBench. Project page: <https://rectified-cfgpp.github.io/>.

## 18 1 Introduction

19 Generative models have seen dramatic advances  
 20 diffusion-based methods now achieve state-of-the-  
 21 art image synthesis by learning to reverse a stochastic  
 22 or deterministic noise process via SDEs/ODEs [36,  
 23 12, 6, 34, 37, 4], combined with scalable architec-  
 24 tures [28, 30] and fast samplers [24, 44] to far out-  
 25 perform earlier GAN approaches [2]. More recently,  
 26 rectified flow models [22, 21] dispense with stochas-  
 27 ticity by learning deterministic vector fields reducing  
 28 generation to an ODE solve yielding stable training  
 29 and faster sampling than diffusion [9], and large-scale  
 30 flow systems like SD3 [7] and Flux [1] outperform  
 31 diffusion-quality images using a fewer function eval-  
 32 uations.

33 An essential advancement in diffusion models is  
 34 classifier-free guidance (CFG) [13], which drastically  
 35 enhances conditional generation quality and enables  
 36 precise alignment of generated samples with textual  
 37 prompts. CFG linearly extrapolates the unconditional  
 38 score toward the conditional score to sharpen adherence to the prompt, at the expense of potential  
 39 instability and generation artifacts. Although CFG is simple and effective for stochastic diffusions, its  
 40 extrapolative nature is problematic in deterministic flows [5]: the trajectory is pulled off the learned  
 41 manifold, producing color blow-outs, warped geometry, and hyperparameter sensitivity (Fig. 2),  
 42 thus limiting practical applicability. Subsequent variants—dynamic thresholding [34], Characteristic  
 43 guidance [43], CFG++ [5], and APG [33] have tried to alleviate these effects, in diffusion models,  
 44 yet a principled, flow-specific solution remains missing.

45 To address these limitations, we introduce Rectified-CFG++, a guidance scheme tailored for  
 46 rectified-flow models. Our key insight is that the geometric structure of RF sampling favors in-  
 47 terpolation, which synergistically combines the stable and deterministic generative trajectories of  
 48 rectified flow models with the powerful conditional generation capabilities of classifier-free guidance.  
 49 At every step, Rectified-CFG++ (i) follows the conditional RF field to keep the sample on the  
 50 transport path, then (ii) applies a scheduled interpolation towards the conditional and unconditional  
 51 field on previously obtained conditional samples. The resulting predictor–corrector integrator (Sec. 3)  
 52 preserves marginal consistency, maintains on-manifold trajectories thereby effectively eliminating  
 53 off-manifold artifacts, and requires no extra networks or optimization. Moreover, we provide a  
 54 theoretical foundation for Rectified-CFG++, and show that it ensures the stability of generated sam-  
 55 ples on the underlying data manifold. We explain the geometric interpretation of Rectified-CFG++,  
 56 and demonstrate how it maintains trajectories within the manifold, thereby preventing the detri-  
 57 mental deviations common to CFG sampling. Extensive experiments on four large text-to-image RF  
 58 backbones—Flux [1], Stable-Diffusion 3/3.5 [7], and Lumina-Next[26]—show that Rectified-CFG++  
 59 consistently outperforms vanilla CFG [13] across FID [11], CLIP-Score [27, 10, 15], ImageRe-  
 60 ward [42], Aesthetic Score [35], and HPS-v2 [40], while reducing artifacts such as oversaturation  
 61 and typographic failure (Sec. 4). We also conduct a subjective study. Qualitative comparisons (Figs. 2  
 62 and 3) reveal smoother intermediate states and sharply improved text alignment. Our contributions  
 63 are summarized as follows:

- 64 • We propose **Rectified-CFG++**, a novel predictor–corrector sampler that uses time-scheduled  
 65 interpolation between conditional and unconditional velocity fields. Our method is parameter-free  
 66 beyond the guidance scale.
- 67 • We provide a detailed theoretical justification including rigorous proofs, and a geometric interpreta-  
 68 tion that our sampler preserves manifold consistency and superior conditioning efficacy.
- 69 • Using diverse datasets and comparison against leading models, we demonstrate that Rectified-  
 70 CFG++ yields better prompt alignment and visual quality than CFG, while mitigating its character-  
 71 istic artifacts in flow-based models.



Figure 2: **Effect of guidance on flow-based models.** (Left) Unguided samples lack structure; (Middle) naive CFG introduces semantic drift and artifacts. (Right) Rectified CFG++ yields detailed and well-aligned outputs.



**Prompt:** A lone anthropomorphic fox in crystalline samurai armor, standing still in a bamboo grove made of glass, glowing runes etched into ...

Figure 3: **Comparison of intermediate denoising steps of CFG and Rectified-CFG++.** Visual progression of decoded latents across 7 sampling steps, starting from  $t=1000$  (top left) to  $t=0$  (top right). While CFG led to artifacts and structural instability early on, Rectified CFG++ maintained on-manifold transitions and preserved fine textures throughout.

72 By bridging the gap between flow-matching ODEs and modern guidance techniques, Rectified-CFG++  
 73 unlocks high-fidelity, *manifold-aware* conditional generation with the efficiency benefits of rectified  
 74 flows.

## 75 2 Preliminaries

76 We review (i) conditional flow-matching (CFM) for generative ODEs and (ii) classifier-free guidance  
 77 (CFG) as typically used with diffusion/flow models. Throughout,  $x \sim p_0$  denotes a data sample,  
 78  $z \sim \mathcal{N}(0, I)$  a Gaussian prior, and  $t \in [0, 1]$  is a time index.

79 **Flow matching models:** CFM [21, 22] learns a velocity field  $v_\theta : \mathbb{R}^d \times [0, 1] \times \mathcal{Y} \rightarrow \mathbb{R}^d$  that  
 80 transports latent states from the prior  $p_1$  to the data distribution  $p_0$ , *conditioned* on an input  $y \in \mathcal{Y}$   
 81 (e.g. a text prompt):

$$\frac{d}{dt} x_t = v_\theta(x_t, t, y), \quad x_1 = z, \quad z \sim p_1. \quad (1)$$

82 A convenient probability path is the *linear* mixture  $p_t = (1-t)p_0 + t p_1$ ; drawing  $(x_0, x_1) \sim (p_0, p_1)$   
 83 yields a closed-form *target* velocity  $u_t(x_t|x_0) = x_1 - x_0$ . Training minimises the conditional  
 84 flow-matching loss [21]:

$$\mathcal{L}_{\text{CFM}}(\theta) = \mathbb{E}_{t, x_0, x_1} \|v_\theta(x_t, t, y) - u_t(x_t|x_0)\|_2^2, \quad (2)$$

85 where  $x_t = (1-t)x_0 + tx_1$ . At inference we numerically integrate (1) deterministically, typically  
 86 with an ordinary differential equation (ODE) Solver [37, 23]. The marginal velocity [21] required  
 87 can be written as:

$$u_t(x_t) = \mathbb{E}_{x_0 \sim p_0} [u_t(x_t|x_0)]. \quad (3)$$

88 **Classifier free guidance for flows:** CFG [13] steers generation towards the condition  $y$  by combining  
 89 the conditional and unconditional velocity fields of a single network trained with randomized null  
 90 conditions  $y = \emptyset$ :

$$\hat{v}_\omega(x_t, t, y; \omega) = (1 - \omega)v_\theta(x_t, t, \emptyset) + \omega v_\theta(x_t, t, y), \quad (4)$$

91 where  $\omega \geq 1$  is the guidance scale that controls text-alignment strength. In (4),  $\omega$  extrapolates guidance  
 92 along  $\Delta v_t^\theta = v_\theta(x_t, t, y) - v_\theta(x_t, t, \emptyset)$ , which often sends trajectories off the learned data manifold,  
 93 producing oversaturated or distorted images [5].

94 **Notation:** For brevity we write  $v_t^c := v_\theta(x_t, t, y)$ ,  $v_t^u := v_\theta(x_t, t, \emptyset)$ ,  $\Delta v_t^\theta := v_t^c - v_t^u$ .  
 95 Standard CFG updates  $x_t$  via the ODE step as  $x_{t-\Delta t} = x_t + \Delta t (v_t^u + \omega \Delta v_t^\theta)$ , which is an affine  
 96 extrapolation in  $\Delta v_t^\theta$ . While flow models offer deterministic, fast sampling, naively plugging (4)  
 97 into the ODE solver inherits the same off-manifold drift observed in diffusion models [5, 33], which  
 98 can lead to divergence because the flow field is integrated without stochastic regularization effect  
 99 of introduced noise in diffusion SDEs. These limitations motivate our Rectified-CFG++ strategy  
 100 introduced in Sec. 3, which replaces the extrapolation term  $\omega \Delta v_t^\theta$  with time-scheduled interpolation  
 101 that preserves the geometry of the learned transport path.

102 **3 Method**

103 In the context of ODE integration, especially  
 104 when the underlying vector field corresponds  
 105 to transport along potentially curved manifolds,  
 106 applying Eq. (4) can lead to significant deviations  
 107 from the true conditional paths learned by  
 108 the model [5, 8, 33]. This often results in vi-  
 109 sual artifacts like oversaturation, semantic drift,  
 110 and structural inconsistencies (see Fig. 2 and  
 111 Fig. 3). To overcome these limitations, we pro-  
 112 pose Rectified-CFG++, which is detailed in Al-  
 113 gorithm 1. Our approach replaces the unstable  
 114 extrapolation of CFG with an adaptive predictor-  
 115 corrector that leverages the geometry of the  
 116 learned conditional flow, while incorporating  
 117 guidance in a controlled manner.

118 **3.1 Rectified-CFG++**

119 The Rectified-CFG++ guidance modifies the velocity used within each step of a numerical ODE  
 120 solver. Instead of directly using the CFG velocity Eq. (4), it constructs an effective velocity  $\hat{v}_{\lambda t}$   
 121 using information from both the current state  $x_t$  and a predicted future state, within time interval  $[t, t - \Delta t/2]$ .

123 **Conditional Predictor:** Specifically, we use the conditional velocity  $v_t^c$  as the predictor step. This  
 124 is crucial because our goal is to generate a sample following the condition  $y$ . Using  $v_t^c$  immediately  
 125 steers the prediction towards the target subspace manifold  $\mathcal{M}_t$ . Using  $v_t^u$  or a CFG-mixed velocity  
 126 here could introduce instability early in the step [33, 8].

$$\tilde{x}_{t-\Delta t/2} \leftarrow x_t + \Delta t/2(v_t^c). \quad (5)$$

127 Geometrically (Fig. 1(Middle)), the intermediate conditional update brings the sample along the  
 128 manifold. This avoids going off-manifold early on in sampling, see Fig. 3.

129 **Correction via Guidance Difference:** Instead of averaging derivatives [3], following [13, 33, 41] we  
 130 compute the difference between conditional and unconditional velocities as in CFG [13],  $\Delta v^\theta$ , but at  
 131 the intermediate predicted point. This term specifically isolates the signal related to the condition  $y$   
 132 in the vicinity of where the trajectory is heading. Evaluating it at  $\tilde{x}_{t-\Delta t/2}$  provides more relevant  
 133 guidance correction as compared to using  $\Delta v_t^\theta$ , especially if the vector field is rapidly changing speed  
 134 or direction:

$$v_{t-\Delta t/2}^c \leftarrow v_\theta(\tilde{x}_{t-\Delta t/2}, t - \Delta t/2, y) \quad (6)$$

$$v_{t-\Delta t/2}^u \leftarrow v_\theta(\tilde{x}_{t-\Delta t/2}, t - \Delta t/2, \emptyset). \quad (7)$$

136 **Interpolative Update:** The final effective velocity  $\hat{v}_{\lambda t}$  anchors the update firmly to the current  
 137 conditional direction  $v_t^c$  and adds a correction based on the predicted guidance need, scaled by a  
 138 weight term. This avoids using the unstable  $v_t^u$  as a base and replaces extrapolation with an adaptive  
 139 correction based on intermediate prediction:

$$\hat{v}_{\lambda t} \leftarrow v_t^c + \alpha(t)(v_{t-\frac{\Delta t}{2}}^c - v_{t-\frac{\Delta t}{2}}^u) \quad (8)$$

140 This structure aims to maintain proximity to the learned conditional flow path, while incorporating  
 141 guidance information ( $\Delta v_{t-\Delta t/2}^\theta$ ) evaluated at a more relevant intermediate point, thereby enhancing  
 142 stability and fidelity as compared to direct CFG [13] extrapolation.

143 **3.2 Theoretical Analysis**

144 Next we provide theoretical justification of the improved stability of Rectified-CFG++. Let  $\psi_t(x_1|y)$   
 145 denote the true trajectory under the ideal conditional velocity  $v_\theta(x_t, t, y)$ , generating the manifold  
 146  $\mathcal{M}_t = \{\psi_t(x_1|y)|x_1 \sim p_1\}$ . In the following, we say that the function  $f$  is Lipschitz continuous on  
 147  $\mathbb{R}$  if  $|f(a) - f(b)| \leq L|a - b|, \forall a, b \in \mathbb{R}$ , where  $L$  is a Lipschitz constant.

Table 1: **Comprehensive Quantitative Evaluation of CFG against Rectified-CFG++ when both are integrated into leading T2I Models on MS-COCO 10K validation samples.** Lower(↓) FID and higher(↑) CLIP, Aesthetic, ImageReward, PickScore, and HPSv2 scores indicate better performance. Best values are highlighted in orange, and second best in gray.

Model	Guidance	FID ↓	CLIP ↑	Aesthetic ↑	ImageReward ↑	PickScore ↑	HPSv2 ↑
Lumina [26]	CFG Rect-CFG++	26.9321 <b>22.4899</b>	0.3511 <b>0.3464</b>	5.8226 <b>5.7755</b>	1.0924 <b>0.9611</b>	0.5867 <b>0.6133</b>	0.2797 <b>0.3004</b>
SD3 [7]	CFG Rect-CFG++	23.8898 <b>23.3945</b>	0.3439 <b>0.3471</b>	5.5465 <b>5.6529</b>	0.9812 <b>1.0009</b>	0.4408 <b>0.5591</b>	0.2751 <b>0.2897</b>
SD3.5 [7]	CFG Rect-CFG++	20.2945 <b>20.2169</b>	0.3506 <b>0.3497</b>	6.155 <b>6.1651</b>	1.0487 <b>1.0796</b>	0.4923 <b>0.5077</b>	0.2933 <b>0.2946</b>
Flux-dev [1]	CFG Rect-CFG++	37.8625 <b>32.2262</b>	0.3351 <b>0.3493</b>	4.7210 <b>5.3251</b>	1.0528 <b>0.9480</b>	0.3248 <b>0.6752</b>	0.2621 <b>0.2996</b>

148 **Assumptions:** **(A1)**  $v_\theta(x, t, y)$  and  $v_\theta(x, t, \emptyset)$  are Lipschitz continuous in  $x$  with constant  $L$ , and  
149 uniformly in continuous  $t$  and  $y$ . **(A2)** The guidance direction magnitude is bounded:  $\|\Delta v_t^\theta(x)\| \leq B$   
150 for all  $(x, t, y) \in \mathbb{R}^3$ , for some  $B \in \mathbb{R}$ . **(A3)** The schedule  $\alpha(t)$  is bounded and integrable. **(A4)**  
151 The conditional velocity magnitude is bounded:  $\|v_t^c(x)\| \leq V_{\max}$  for all  $(x, t, y) \in \mathbb{R}^3$ , for some  
152  $V_{\max} \in \mathbb{R}$ .

153 We begin by analyzing how the guidance term evaluated at an intermediate point relates to the  
154 guidance term at the current point ( $t$ ).

**Lemma 3.1** (Stability of Predicted Guidance Direction). *Under assumptions (A1) and (A4), the guidance direction  $\Delta v_{t-\Delta t/2}^\theta$  computed at the predicted state  $\tilde{x}_{t-\Delta t/2}$  differs from the guidance direction  $\Delta v_t^\theta(x_t)$  at the current state by an amount proportional to the step size  $\Delta t$ :*

$$\|\Delta v_{t-\Delta t/2}^\theta - \Delta v_t^\theta(x_t)\| \leq L V_{\max} \Delta t.$$

155 *Proof.* See Appendix A.2. □

156 This lemma suggests that for sufficiently small step sizes, the guidance direction computed at the  
157 predicted point  $\tilde{x}_{t-\Delta t/2}$  is close to the direction at the current point  $x_t$ , thereby ensuring the correction  
158 term is relevant. Next, we quantify the deviation introduced by the guidance correction in a single  
159 step, as compared to following the pure conditional flow.

**Proposition 1** (Bounded Single-Step Perturbation). *Let  $\hat{x}_{t-1}$  be the result of a single Rectified-CFG++ step from  $x_t$ . Let  $\tilde{x}_{t-1}$  be the result of a pure conditional Euler step. Under assumption (A2), the deviation is:*

$$\|\hat{x}_{t-1} - \tilde{x}_{t-1}\| \leq \alpha(t) B \Delta t.$$

160 *Proof.* See Appendix A.3. □

161 This proposition implies that the per-step deviation from the conditional path is directly controlled  
162 by the weight  $\alpha(t)$  and the bound  $B$  imposed on the guidance field magnitude, scaled by the step  
163 size  $\Delta t$ . Thus, the Rectified-CFG++ trajectory stays within a bounded tubular neighborhood of the  
164 ideal manifold  $\mathcal{M}_t$ . The size of this neighborhood is controlled by the guidance strength  $\alpha(t)$  and  
165 by the guidance field bound  $B$ . This analysis shows that, unlike standard CFG whose extrapolative  
166 nature can lead to divergence, the trajectories of Rectified-CFG++ are anchored to  $v_t^c$ . Applying  
167 a controlled correction based on  $\Delta v_{t-\Delta t/2}^\theta$  with a guidance weight  $\alpha(t)$  ensures that the trajectory  
168 remains boundedly close to the target conditional flow path. This mathematical stability ensures to  
169 the empirical robustness and artifact reduction observed our results.

## 170 4 Experiments

171 In this section, we present a comprehensive empirical evaluation of Rectified-CFG++ for text-to-  
172 image (T2I) generation using large-scale models. Our experiments aim to rigorously demonstrate the  
173 effectiveness of our approach at improving text-image alignment, color fidelity, and the preservation  
174 of fine details, generating high-quality samples while expending comparable inference costs as  
175 competing baseline methods.

176 **Evaluation Metrics:** To provide a multifaceted assessment of generated image quality and prompt  
177 adherence, we employed a suite of established metrics. We measured perceptual image quality and

Table 2: **Quantitative Evaluation on T2I-CompBench.** Evaluated across Color, Shape, Texture, and Spatial metrics. Rectified-CFG++ improves consistently across all dimensions.

Model	Color $\uparrow$	Shape $\uparrow$	Texture $\uparrow$	Spatial $\uparrow$
Lumina [26]	0.7358	0.6898	0.7365	0.3586
w/ Rect-CFG++	<b>0.7767</b>	<b>0.7042</b>	<b>0.6856</b>	<b>0.3608</b>
SD3 [7]	0.7658	0.5698	0.7270	0.3199
w/ Rect-CFG++	<b>0.8041</b>	<b>0.5778</b>	<b>0.7362</b>	<b>0.3306</b>
SD3.5 [7]	0.7698	0.5792	0.7413	0.2856
w/ Rect-CFG++	<b>0.7770</b>	<b>0.6014</b>	<b>0.7627</b>	<b>0.2909</b>
Flux-dev [1]	0.6132	0.4152	0.5928	0.2488
w/ Rect-CFG++	<b>0.7728</b>	<b>0.5018</b>	<b>0.6705</b>	<b>0.2790</b>

Table 3: **Quantitative Comparison of Guidance Strategies on MS-COCO 1K.** We evaluated standard guidance methods against Rectified-CFG++ using FID ( $\downarrow$ ), IS ( $\uparrow$ ), Precision ( $\uparrow$ ), and Recall ( $\uparrow$ ).

Guidance	FID $\downarrow$	ImageReward $\uparrow$	CLIP $\uparrow$	HPSv2 $\uparrow$
SD3.5	77.3049	0.3852	0.3260	0.2421
w/ CFG	67.7133	1.0530	<b>0.3515</b>	0.2941
w/ CFG-Zero*	68.3909	0.9947	0.3458	0.2879
w/ APG	67.2311	1.0748	0.3513	0.2935
w/ Rect-CFG++	<b>67.1495</b>	<b>1.0845</b>	<b>0.3506</b>	<b>0.2959</b>

realism using the Fréchet Inception Distance (FID) [11], and we quantified text-image semantic alignment is using CLIP-Score [27, 10, 15]. Furthermore, to capture aspects related to human preferences, visual aesthetics, and overall quality, we utilize ImageReward [42], PickScore [18, 38], HPSv2 [40], and Aesthetic Score [35]. These metrics collectively allow for a thorough evaluation of the generated images from different perspectives.

**Datasets and Baselines:** We conducted objective model comparison on standard T2I benchmark datasets. Specifically, we used subsets of the MS-COCO dataset [20, 5], comprising 10,000 and 1,000 image-text pairs (referred to as MS-COCO 10K and MS-COCO 1K, respectively). We also used a subset of 1,000 image-text pairs from LAION-Aesthetic [35] (LAION-Aesthetic 1K) and the 1,000 prompts from Pick-A-Pic [18]. To demonstrate the broad applicability of Rectified-CFG++, we integrated it into and evaluate it on several state-of-the-art flow-based T2I foundation models: Stable Diffusion 3 [7], Stable Diffusion 3.5 [7], Flux [1], and Lumina [26]. These models are representative of current advancements in flow-based generative architectures.

**Implementation Details:** All experiments were performed using a single NVIDIA A100 40GB GPU. When using our proposed method, Rectified-CFG++, we determined a set of effective hyperparameters which were kept consistent across all datasets and when integrated into baseline models. For all the compared methods, we utilized the default settings and configurations as reported in their original publications to ensure fair comparisons. Further detailed information regarding the experimental setup and hyperparameter settings can be found in Appendix D.1.

## 4.1 Text-to-Image Generation Evaluation

### 4.1.1 Quantitative Evaluation

We first assess performance using established quantitative metrics. Table 3 provides a comparison on MS-COCO-1K against several guidance strategies: standard CFG [13], CFG++ [5], APG [33], and CFG-Zero\* [8]. Rectified-CFG++ consistently outperformed the other strategies across all metrics on SD3.5 [7]. The results of a more comprehensive evaluation across multiple foundation models on MS-COCO-10K are given in Table 1. These outcomes clearly demonstrate the efficacy of using Rectified-CFG++ when combined with leading text-to-image models. As compared to standard CFG integrated with the same base models, our method consistently improves scores across nearly all metrics. Notably, Rectified-CFG++ significantly lowers FID (indicating higher image fidelity) while simultaneously enhancing scores related to text alignment and human preference (CLIP, ImageReward, PickScore, HPSv2), as highlighted by the best in orange and second-best in gray values. For instance, on Lumina-Next, FID drops from 26.93 to 22.49, and on Flux, FID improves substantially from 37.86 to 32.23, accompanied by consistent gains in human preference metrics. Furthermore, we evaluated performance on T2I-CompBench [14]. As shown in Table 2, Rectified-CFG++ consistently improves text-to-image model performance than does baseline CFG across all four attribute dimensions, indicating enhanced capability at generating images that accurately reflect complex compositional instructions. We provide more experimental results in Appendix D.3.

### 4.1.2 Intermediate Sampling Analysis

To understand the convergence dynamics and efficiency of Rectified-CFG++, we analyzed its generation quality at intermediate sampling steps. As may be observed in Fig. 3, standard CFG often introduces artifacts like oversaturation and high contrast early in the sampling process, and sometimes



Figure 4: T2I results from Flux [1] across pick-a-pic [18] prompts.

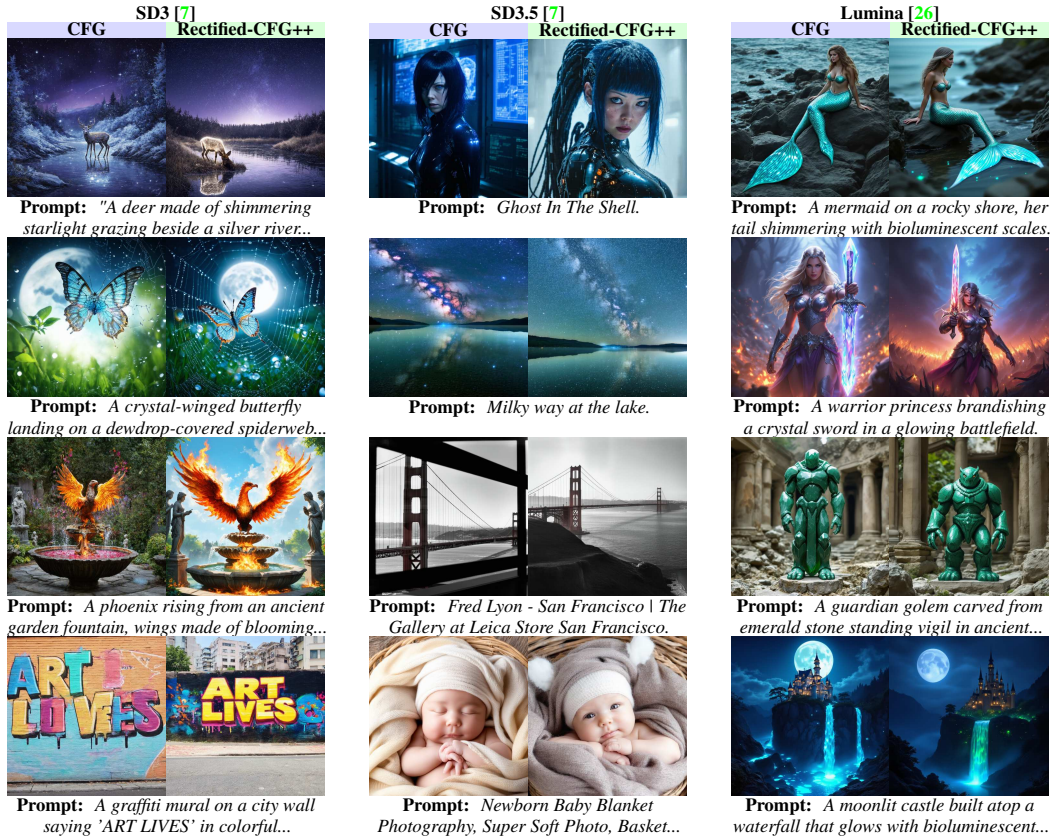


Figure 6: **Comparison of CFG vs Rectified-CFG++ combined with SD3/3.5 [7] and Lumina [26] with diverse prompts.** Rectified-CFG++ consistently better enhance semantic alignment, compositional balance, and generative fidelity across models and scenes.

219 significantly deviates from the target manifold. By contrast, Rectified-CFG++ maintains stable  
220 generation quality throughout the process. More detailed visualization examples are provided in  
221 Appendix D.

#### 222 4.1.3 Qualitative Evaluation

223 Qualitative comparisons further illuminate the advantages of Rectified-CFG++. Fig. 4 shows generated  
224 text-to-image examples from the Flux [1] model combined with the default Conditional flow ,  
225 Standard CFG , and Rectified-CFG++ . Our method produced images having better semantic  
226 quality, alignment, details, and overall composition with less visible artifacts. Fig. 6 extends this



Figure 7: **Rectified-CFG++ enhances text generation quality.** It consistently improves the accuracy, legibility, and semantic alignment of text-to-image models as compared to standard CFG.

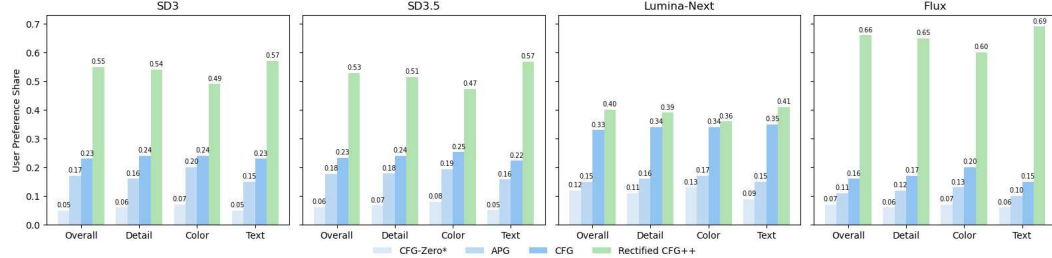


Figure 8: User study results comparing various guidance. The user preference ratio indicates the percentage of participants that preferred images created using Rectified-CFG++ over those created using CFG in terms of detail preservation, color consistency, and prompt alignment.

comparison across SD3 [7], SD3.5 [7], and Lumina [26] using diverse curated prompts. Again, Rectified-CFG++ consistently better enhanced semantic alignment, compositional balance, and overall generative fidelity across all models and prompt types. Fig. 5 visually compares different guidance methods. While standard CFG often suffers from oversaturation and misalignment, and other methods like APG [33] and CFG-Zero\* [8] offer partial improvements but compromise on detail or geometric accuracy, Rectified-CFG++ reliably yields more faithful, high-quality output.

**Text Legibility:** Importantly, Rectified-CFG++ significantly improves the rendering of text intent within images, a known challenge of diffusion models. As illustrated in Fig. 7, prompts containing specific text like “CyberCore Café” or “Feathered Conspiracies” are rendered with much greater accuracy and legibility using Rectified-CFG++. The textual intent is clearer, better integrated into each scene, and more semantically correct. Additional examples demonstrating improved text rendering are provided in Appendix D.4.

#### 4.1.4 User Study

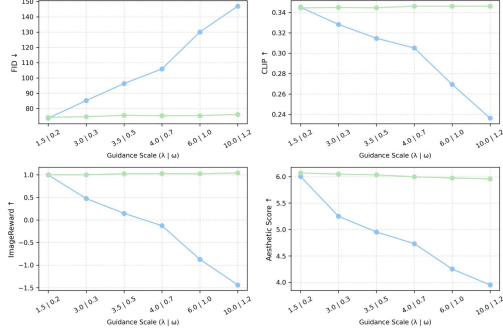
To further validate Rectified-CFG++’s performance, we conducted a user study. For a given prompt and base model, participants were presented with four images generated using standard CFG [13], APG [33], CFG-Zero\* [8], and Rectified-CFG++, each set presented in a randomized order. They were asked to select the best image based on the following criteria: *Image Detail*, *Color Naturalness and Consistency*, and *Prompt Alignment (including text legibility)*. Figure 8 displays the user preference ratios, indicating the preference of Rectified-CFG++ over the other guidance methods. More detail in Appendix D.2.

## 4.2 Ablation Studies

**Guidance Scale and Sampling Steps:** We investigated the impact of varying the guidance scales and the number of sampling steps (NFEs). Fig. 9(a) shows FID, CLIP, ImageReward and Aesthetic scores plotted against the guidance scale parameters, i.e.  $\lambda$  or  $\omega$ . Rectified-CFG++ maintained high

Table 4: Computational cost comparison of standard CFG and Rectified-CFG++.

Resolution	Guidance	NFEs	FLOPs (G) ↓	Runtime (s) ↓
512x512	CFG	28	$0.61 \times 10^6$	5.3148
	Rect-CFG++	20	$0.61 \times 10^6$	5.3506
1024x1024	CFG	28	$2.1 \times 10^6$	16.2617
	Rect-CFG++	20	$2.1 \times 10^6$	17.8804

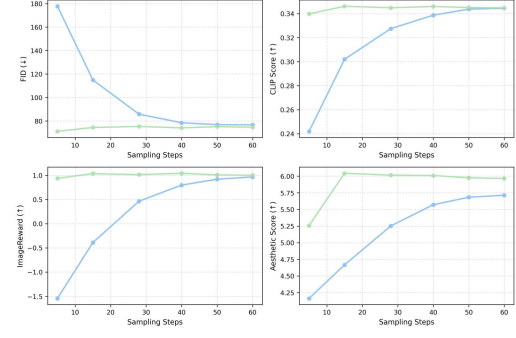


((a)) Effect of guidance scale ( $\lambda|\omega$ ).

Figure 9: Ablation study across guidance scales and sampling steps. Assessed using FID(upper left), CLIP(upper right), ImageReward(lower left), and Aesthetic Scores (lower right) for both (a) and (b).

Table 5: Ablation study of Rectified-CFG++ components on MS-COCO 1K samples.

Configuration	FID ↓	CLIP ↑	HPSv2 ↑	Aesthetic ↑
w/ Unconditional	91.1180	0.1439	0.1870	6.1049
w/o Predictor	73.6981	0.3410	0.2969	6.1064
w/o Corrector	74.6545	0.3414	0.2975	6.1047
<b>Rectified-CFG++</b>	<b>72.9745</b>	<b>0.3446</b>	<b>0.2995</b>	<b>6.1587</b>



((b)) Comparison across sampling steps (NFEs).

251 performance and stability across a wide range of scales, whereas standard CFG [13] swiftly degraded.  
252 This indicates that CFG [13] pushes samples further off-manifold. Figure 9(b) illustrates performance  
253 relative to the number of sampling steps (NFEs). Rectified-CFG++ consistently outperforms standard  
254 CFG, achieving better scores even with significantly fewer steps. This reinforces the findings in  
255 Section 4.1.2 and underscores the efficiency gains enabled by our method.

256 **Component Analysis:** To isolate the contributions of the key components of Rectified-CFG++, we  
257 conducted an ablation study on MS-COCO 1K using FID, CLIP, HPSv2, and Aesthetic Score as  
258 shown in Table 5. The outcomes show that removing any of the studied components leads to degraded  
259 performance compared to the complete Rectified-CFG++ method. The configuration combining both  
260 the predictor and corrector steps achieved the best overall scores, validating the effectiveness of our  
261 integrated design.

262 **Computational Efficiency:** Beyond generation quality, practical deployment requires computational  
263 efficiency. As demonstrated in our intermediate sampling analysis (Section 4.1.2) and ablation studies  
264 Rectified-CFG++ achieves high-quality results using the same number or fewer sampling steps  
265 (NFEs) as compared to standard CFG. Table 4 provides a direct comparison of text-to-image model  
266 performance using Rectified-CFG++ against standard CFG, where both models’ outcomes were  
267 assessed as having similar FID scores (74.47 vs. 76.88 on COCO-1K, respectively). In this scenario,  
268 Rectified-CFG++ required fewer NFEs, which translates to lower computational cost, reducing both  
269 total FLOPs and inference runtime. These efficiency gains make Rectified-CFG++ more suitable for  
270 applications demanding faster generation or operating under resource constraints.

## 271 5 Conclusion and Discussion

272 We introduced **Rectified-CFG++**, a predictor–corrector guidance for text-to-image generative models  
273 that first follows the conditional velocity, then applies a weighted interpolation. When combined with  
274 leading flow-based foundation models, Rectified-CFG++ consistently improved performance against  
275 all quality measurements. Furthermore, Rectified-CFG++ demonstrated greater stability across  
276 varying guidance scales, mitigating artifact and quality degradation issues frequently encountered  
277 when using CFG. A user study confirmed perceptual gains in detail, colour fidelity and text alignment  
278 when using Rectified-CFG++. Because Rectified-CFG++ is training-free and adds negligible compute,  
279 it can serve as a drop-in upgrade of existing flow-matching generators. Future work will explore  
280 extensions to video and 3-D diffusion, and integration with preference-based reinforcement guidance  
281 models.

282 **References**

- 283 [1] Black Forest Labs. Flux. <https://github.com/black-forest-labs/flux>, 2024. 2, 5, 6, 7, 15, 17,  
284 18, 20, 21, 22, 26
- 285 [2] Andrew Brock, Jeff Donahue, and Karen Simonyan. Large scale gan training for high fidelity natural  
286 image synthesis. *arXiv preprint arXiv:1809.11096*, 2018. 2
- 287 [3] John C Butcher. Differential equations, numerical methods and algebraic analysis. In *B-Series: Algebraic*  
288 *Analysis of Numerical Methods*, pages 1–37. Springer, 2021. 4
- 289 [4] Ricky T. Q. Chen, Yulia Rubanova, Jesse Bettencourt, and David K. Duvenaud. Neural ordinary differential  
290 equations. In *Advances in Neural Information Processing Systems (NeurIPS)*, pages 6571–6583, 2018. 2,  
291 17
- 292 [5] Hyungjin Chung, Jeongsol Kim, Geon Yeong Park, Hyelin Nam, and Jong Chul Ye. Cfg++: Manifold-  
293 constrained classifier free guidance for diffusion models. *arXiv preprint arXiv:2406.08070*, 2024. 2, 3, 4,  
294 6, 17
- 295 [6] Prafulla Dhariwal and Alex Nichol. Diffusion models beat gans on image synthesis. In *Advances in Neural*  
296 *Information Processing Systems (NeurIPS)*, pages 8780–8794, 2021. 2, 17
- 297 [7] Patrick Esser, Sumith Kulal, Andreas Blattmann, Rahim Entezari, Jonas Müller, Harry Saini, Yam Levi,  
298 Dominik Lorenz, Axel Sauer, Frederic Boesel, et al. Scaling rectified flow transformers for high-resolution  
299 image synthesis. In *Forty-first international conference on machine learning*, 2024. 2, 5, 6, 7, 8, 17, 18, 20,  
300 21, 22, 23, 24, 25, 28, 29
- 301 [8] Weichen Fan, Amber Yijia Zheng, Raymond A Yeh, and Ziwei Liu. Cfg-zero\*: Improved classifier-free  
302 guidance for flow matching models. *arXiv preprint arXiv:2503.18886*, 2025. 4, 6, 8, 16, 17, 18
- 303 [9] Will Grathwohl, Ricky T. Q. Chen, Jesse Bettencourt, Ilya Sutskever, and David Duvenaud. Ffjord:  
304 Free-form continuous dynamics for scalable reversible generative models. In *International Conference on*  
305 *Learning Representations (ICLR)*, 2019. 2, 17
- 306 [10] Jack Hessel, Ari Holtzman, Maxwell Forbes, Ronan Le Bras, and Yejin Choi. Clipscore: A reference-free  
307 evaluation metric for image captioning. *arXiv preprint arXiv:2104.08718*, 2021. 2, 6
- 308 [11] Martin Heusel, Hubert Ramsauer, Thomas Unterthiner, Bernhard Nessler, and Sepp Hochreiter. Gans  
309 trained by a two time-scale update rule converge to a local nash equilibrium. *Advances in neural information*  
310 *processing systems*, 30, 2017. 2, 6
- 311 [12] Jonathan Ho, Ajay Jain, and Pieter Abbeel. Denoising diffusion probabilistic models. *Advances in neural*  
312 *information processing systems*, 33:6840–6851, 2020. 2, 17
- 313 [13] Jonathan Ho and Tim Salimans. Classifier-free diffusion guidance. *arXiv preprint arXiv:2207.12598*, 2022.  
314 2, 3, 4, 6, 8, 9, 15, 17, 18, 22
- 315 [14] Kaiyi Huang, Chengqi Duan, Kaiyue Sun, Enze Xie, Zhenguo Li, and Xihui Liu. T2i-compbench++: An  
316 enhanced and comprehensive benchmark for compositional text-to-image generation. *IEEE Transactions*  
317 *on Pattern Analysis and Machine Intelligence*, 2025. 6
- 318 [15] Gabriel Ilharco, Mitchell Wortsman, Ross Wightman, Cade Gordon, Nicholas Carlini, Rohan Taori, Achal  
319 Dave, Vaishaal Shankar, Hongseok Namkoong, John Miller, et al. Openclip. *If you use this software,*  
320 *please cite it as below*, 7, 2021. 2, 6
- 321 [16] Tero Karras, Miika Aittala, Tuomas Kynkänniemi, Jaakko Lehtinen, Timo Aila, and Samuli Laine.  
322 Guiding a diffusion model with a bad version of itself. *Advances in Neural Information Processing Systems*,  
323 37:52996–53021, 2024. 17
- 324 [17] Durk P Kingma and Prafulla Dhariwal. Glow: Generative flow with invertible 1x1 convolutions. *Advances*  
325 *in neural information processing systems*, 31, 2018. 17
- 326 [18] Yuval Kirstain, Adam Polyak, Uriel Singer, Shahbuland Matiana, Joe Penna, and Omer Levy. Pick-a-  
327 pic: An open dataset of user preferences for text-to-image generation. *Advances in Neural Information*  
328 *Processing Systems*, 36:36652–36663, 2023. 6, 7, 18
- 329 [19] Tuomas Kynkänniemi, Miika Aittala, Tero Karras, Samuli Laine, Timo Aila, and Jaakko Lehtinen.  
330 Applying guidance in a limited interval improves sample and distribution quality in diffusion models. *arXiv*  
331 *preprint arXiv:2404.07724*, 2024. 17

- 332 [20] Tsung-Yi Lin, Michael Maire, Serge Belongie, James Hays, Pietro Perona, Deva Ramanan, Piotr Dollár,  
 333 and C Lawrence Zitnick. Microsoft coco: Common objects in context. In *Computer vision–ECCV 2014:*  
 334 *13th European conference, zurich, Switzerland, September 6–12, 2014, proceedings, part v 13*, pages  
 335 740–755. Springer, 2014. 6, 18
- 336 [21] Yaron Lipman, Ricky T. Q. Chen, Heli Ben-Hamu, Maximilian Nickel, and Matthew Le. Flow matching  
 337 for generative modeling. In *The Eleventh International Conference on Learning Representations*, 2023. 2,  
 338 3, 17
- 339 [22] Yiming Liu and Yaron Lipman. Rectified flow: A marginal preserving approach to optimal transport. In  
 340 *International Conference on Machine Learning (ICML)*, pages 21607–21631. PMLR, 2023. 2, 3, 17
- 341 [23] Cheng Lu, Yuhao Zhou, Fan Bao, Jianfei Chen, Chongxuan Li, and Jun Zhu. Dpm-solver: A fast ode  
 342 solver for diffusion probabilistic model sampling in around 10 steps. *Advances in Neural Information*  
 343 *Processing Systems*, 35:5775–5787, 2022. 3
- 344 [24] Artem Lukoianov, Haitz Sáez de Ocáriz Borde, Kristjan Greenewald, Vitor Guizilini, Timur Bagautdinov,  
 345 Vincent Sitzmann, and Justin M Solomon. Score distillation via reparametrized ddim. *Advances in Neural*  
 346 *Information Processing Systems*, 37:26011–26044, 2024. 2
- 347 [25] Alex Nichol, Prafulla Dhariwal, Aditya Ramesh, Pranav Shyam, Pamela Mishkin, Bob McGrew, Ilya  
 348 Sutskever, and Mark Chen. Glide: Towards photorealistic image generation and editing with text-guided  
 349 diffusion models. In *International Conference on Machine Learning (ICML)*, pages 16784–16804. PMLR,  
 350 2022. 17
- 351 [26] Qi Qin, Le Zhuo, Yi Xin, Ruoyi Du, Zhen Li, Bin Fu, Yiting Lu, Jiakang Yuan, Xinyue Li, Dongyang  
 352 Liu, et al. Lumina-image 2.0: A unified and efficient image generative framework. *arXiv preprint*  
 353 *arXiv:2503.21758*, 2025. 2, 5, 6, 7, 8, 17, 18, 20, 21, 22, 27
- 354 [27] Alec Radford, Jong Wook Kim, Chris Hallacy, Aditya Ramesh, Gabriel Goh, Sandhini Agarwal, Girish  
 355 Sastry, Amanda Askell, Pamela Mishkin, Jack Clark, et al. Learning transferable visual models from  
 356 natural language supervision. In *International conference on machine learning*, pages 8748–8763. PmLR,  
 357 2021. 2, 6
- 358 [28] Aditya Ramesh, Prafulla Dhariwal, Alex Nichol, Casey Chu, and Mark Chen. Hierarchical text-conditional  
 359 image generation with clip latents. *arXiv preprint arXiv:2204.06125*, 2022. 2
- 360 [29] Aditya Ramesh, Mikhail Pavlov, Gabriel Goh, Scott Gray, Chelsea Voss, Alec Radford, Mark Chen, and  
 361 Ilya Sutskever. Zero-shot text-to-image generation. In *International conference on machine learning*,  
 362 pages 8821–8831. Pmlr, 2021. 17
- 363 [30] Robin Rombach, Andreas Blattmann, Dominik Lorenz, Patrick Esser, and Björn Ommer. High-resolution  
 364 image synthesis with latent diffusion models. In *Proceedings of the IEEE/CVF Conference on Computer*  
 365 *Vision and Pattern Recognition (CVPR)*, pages 10684–10695, 2022. 2, 17
- 366 [31] Negar Rostamzadeh, Emily Denton, and Linda Petrini. Ethics and creativity in computer vision. *arXiv*  
 367 *preprint arXiv:2112.03111*, 2021. 21
- 368 [32] Seyedmorteza Sadat, Jakob Buhmann, Derek Bradley, Otmar Hilliges, and Romann M Weber. Cads:  
 369 Unleashing the diversity of diffusion models through condition-annealed sampling. *arXiv preprint*  
 370 *arXiv:2310.17347*, 2023. 17
- 371 [33] Seyedmorteza Sadat, Otmar Hilliges, and Romann M Weber. Eliminating oversaturation and artifacts  
 372 of high guidance scales in diffusion models. In *The Thirteenth International Conference on Learning*  
 373 *Representations*, 2024. 2, 3, 4, 6, 8, 17, 18
- 374 [34] Chitwan Saharia, William Chan, Saurabh Saxena, Lala Li, Jay Whang, Emily L Denton, Kamyar  
 375 Ghasemipour, Raphael Gontijo Lopes, Burcu Karagol Ayan, Tim Salimans, et al. Photorealistic text-to-  
 376 image diffusion models with deep language understanding. *Advances in neural information processing*  
 377 *systems*, 35:36479–36494, 2022. 2, 17
- 378 [35] Christoph Schuhmann. LAION-Aesthetics. <https://laion.ai/blog/laion-aesthetics/>, 2022.  
 379 Accessed: 2023-11-10. 2, 6
- 380 [36] Jascha Sohl-Dickstein, Eric Weiss, Niru Maheswaranathan, and Surya Ganguli. Deep unsupervised  
 381 learning using nonequilibrium thermodynamics. In *International conference on machine learning*, pages  
 382 2256–2265. pmlr, 2015. 2

- 383 [37] Yang Song, Jascha Sohl-Dickstein, Diederik P Kingma, Abhishek Kumar, Stefano Ermon, and Ben Poole.  
384 Score-based generative modeling through stochastic differential equations. In *International Conference on*  
385 *Learning Representations (ICLR)*, 2020. 2, 3, 16
- 386 [38] Bram Wallace, Meihua Dang, Rafael Rafailov, Linqi Zhou, Aaron Lou, Senthil Purushwalkam, Stefano  
387 Ermon, Caiming Xiong, Shafiq Joty, and Nikhil Naik. Diffusion model alignment using direct preference  
388 optimization. In *Proceedings of the IEEE/CVF Conference on Computer Vision and Pattern Recognition*,  
389 pages 8228–8238, 2024. 6
- 390 [39] Xi Wang, Nicolas Dufour, Nefeli Andreou, Marie-Paule Cani, Victoria Fernández Abrevaya, David  
391 Picard, and Vicky Kalogeiton. Analysis of classifier-free guidance weight schedulers. *arXiv preprint*  
392 *arXiv:2404.13040*, 2024. 17
- 393 [40] Xiaoshi Wu, Yiming Hao, Keqiang Sun, Yixiong Chen, Feng Zhu, Rui Zhao, and Hongsheng Li. Human  
394 preference score v2: A solid benchmark for evaluating human preferences of text-to-image synthesis. *arXiv*  
395 *preprint arXiv:2306.09341*, 2023. 2, 6
- 396 [41] Mengfei Xia, Nan Xue, Yujun Shen, Ran Yi, Tieliang Gong, and Yong-Jin Liu. Rectified diffusion guidance  
397 for conditional generation. *arXiv preprint arXiv:2410.18737*, 2024. 4, 17
- 398 [42] Jiazheng Xu, Xiao Liu, Yuchen Wu, Yuxuan Tong, Qinkai Li, Ming Ding, Jie Tang, and Yuxiao Dong.  
399 Imagereward: Learning and evaluating human preferences for text-to-image generation. *Advances in*  
400 *Neural Information Processing Systems*, 36:15903–15935, 2023. 2, 6
- 401 [43] Candi Zheng and Yuan Lan. Characteristic guidance: Non-linear correction for diffusion model at large  
402 guidance scale. *arXiv preprint arXiv:2312.07586*, 2023. 2, 17
- 403 [44] Hongkai Zheng, Weili Nie, Arash Vahdat, Kamyar Azizzadenesheli, and Anima Anandkumar. Fast  
404 sampling of diffusion models via operator learning. In *International conference on machine learning*,  
405 pages 42390–42402. PMLR, 2023. 2

---

# Appendix

---

407 This supplementary material justifies the theoretical claims stated in the main paper, supporting the  
 408 mathematical soundness and practical robustness of Rectified-CFG++. Here is the outline of the  
 409 supplementary material:

- 410     • Proofs and Additional Derivations.
- 411     • Rectified-CFG++ Interpretation.
- 412     • Related Work.
- 413     • Additional Experiments.
- 414     • Failure Cases and Limitations.
- 415     • Ethics Statement.
- 416     • Broader Impact Statement.
- 417     • Prompt List

418 **A Proofs and Additional Derivations**

419 **A.1 Manifold Preserving Property of the Rectified-CFG++**

420 Throughout, let  $\mathcal{M}_t \subset \mathbb{R}^d$  denote the (latent) data manifold at time  $t \in [0, 1]$  and assume the network  
 421  $v_\theta$  has been trained with the conditional flow-matching objective (Eq. (2)). Consequently, both the  
 422 conditional and unconditional velocity fields are tangent to  $\mathcal{M}_t$  at every point:

$$\underbrace{v_t^c}_{v_\theta(x_t, t, y)} \in T_{x_t} \mathcal{M}_t, \quad \underbrace{v_t^u}_{v_\theta(x_t, t, \emptyset)} \in T_{x_t} \mathcal{M}_t. \quad (\text{A.1})$$

423 Recall the linear probability path  $\mathcal{M}_t = \{(1-t)x_0 + tx_1 \mid x_0 \sim p_0, x_1 \sim \mathcal{N}(0, I)\}$  and let  
 424  $u_t(x_t | x_0) = x_1 - x_0$  be the *target velocity*. For any  $x_t \in \mathcal{M}_t$  there exists a latent pair  $(x_0, x_1)$  such  
 425 that  $x_t = (1-t)x_0 + tx_1$ .

426 **Lemma A.1 (Manifold-Faithful Corrector).** *Let  $x_t \in \mathcal{M}_t$ . Perform one Rectified-CFG++ step with  
 427 step size  $\Delta t > 0$ , with initial predictor update as  $x_{t-\frac{\Delta t}{2}}$  and corrector guidance as  $\hat{v}_t$  giving the  
 428 final update as  $x_{t-\Delta t} = \text{ODEUpdate}(x_t, t, \hat{v}_t)$ . Assume  $\|v_\tau^c\|, \|v_\tau^u\| \leq L$  for  $\tau \in [t - \frac{\Delta t}{2}, t]$ . Assume  
 429 the network is  $\varepsilon$ -accurate, i.e.  $\|v_\tau^c - u_\tau\| \leq \varepsilon$  and  $\|v_\tau^u - u_\tau\| \leq \varepsilon$  for every  $\tau \in [t - \frac{\Delta t}{2}, t]$ . Then,  
 430 for sufficiently small  $\Delta t$*

$$\text{dist}(x_{t-\Delta t}, \mathcal{M}_{t-\Delta t}) \leq \underbrace{C\varepsilon}_{\text{training error}} \underbrace{\Delta t}_{\text{numerical error}}. \quad (9)$$

431 **Proof.** On  $\mathcal{M}_{t-\Delta t}$ . For the latent pair  $(x_0, x_1)$  that generates  $x_t$ , define:

$$x_{t-\Delta t}^* = (1 - (t - \Delta t))x_0 + (t - \Delta t)x_1 = x_t + \Delta t u_t(x_t | x_0)$$

432 Since flows are in tangent from A.1, we have  $v_\tau^c, v_\tau^u \in T_{x_\tau} \mathcal{M}_\tau$ ; hence their linear combination  $\hat{v}_t$   
 433 also lies in  $T_{x_{t-\frac{\Delta t}{2}}} \mathcal{M}_{t-\frac{\Delta t}{2}}$ . Therefore the corrector displacement is tangent to  $\mathcal{M}_{t-\frac{\Delta t}{2}}$ . Rewriting  
 434 the corrector guidance with true velocity  $u_t$ :

$$\hat{v}_t = u_t + (v_t^c - u_t) + \alpha(t)(v_{t-\frac{\Delta t}{2}}^c - u_t) - \alpha(t)(v_{t-\frac{\Delta t}{2}}^u - u_t).$$

435 The  $\varepsilon$ -accuracy assumption implies  $\|\hat{v}_t - u_t\| \leq (1 + 2\alpha_{\max})\varepsilon$ . Hence,

$$\|x_{t-\Delta t} - x_{t-\Delta t}^*\| = \Delta t \|\hat{v}_t - u_t\| \leq (1 + 2\alpha_{\max})\varepsilon \Delta t. \quad (\text{A.2})$$

436 Because  $x_{t-\Delta t}^* \in \mathcal{M}_{t-\Delta t}$ , the left-hand side of (A.2) is an *upper bound* on  $\text{dist}(x_{t-\Delta t}, \mathcal{M}_{t-\Delta t})$ ,  
 437 completing the proof.

438 **A.2 Proof of Lemma 3.1**

**Lemma A.2** (Stability of Predicted Guidance Direction). *Under assumptions (A1) and (A4), the guidance direction  $\Delta v_{t-\Delta t/2}^\theta$  computed at the predicted state  $\tilde{x}_{t-\Delta t/2}$  differs from the guidance direction  $\Delta v_t^\theta(x_t)$  at the current state by an amount proportional to the step size  $\Delta t/2$ :*

$$\|\Delta v_{t-\Delta t/2}^\theta - \Delta v_t^\theta(x_t)\| \leq LV_{\max}\Delta t.$$

439 *Proof.* Let  $\tilde{x} = \tilde{x}_{t-\Delta t/2} = x_t + \Delta tv_t^c/2$ . By definition,  $\Delta v_{t-\Delta t/2}^\theta = v^c(\tilde{x}) - v^u(\tilde{x})$  and  $\Delta v_t^\theta =$   
440  $v^c(x_t) - v^u(x_t)$ . We want to bound  $\|\Delta v_{t-\Delta t/2}^\theta - \Delta v_t^\theta\|$ :

$$\begin{aligned} \|\Delta v_{t-\Delta t/2}^\theta - \Delta v_t^\theta\| &= \|(v_t^c(\tilde{x}) - v_t^u(\tilde{x})) - (v_t^c(x_t) - v_t^u(x_t))\| \\ &= \|(v_t^c(\tilde{x}) - v_t^c(x_t)) - (v_t^u(\tilde{x}) - v_t^u(x_t))\| \\ &\quad (\text{Applying Triangle Inequality}) \\ &\leq \|v_t^c(\tilde{x}) - v_t^c(x_t)\| + \|v_t^u(\tilde{x}) - v_t^u(x_t)\| \end{aligned}$$

441 By assumption (A1),  $v_t^c$  and  $v_t^u$  are Lipschitz continuous with constant  $L$ :

$$\begin{aligned} \|\Delta v_{t-\Delta t/2}^\theta - \Delta v_t^\theta\| &\leq L\|\tilde{x} - x_t\| + L\|\tilde{x} - x_t\| \\ &= 2L\|\tilde{x} - x_t\|. \end{aligned}$$

Substitute the definition of  $\tilde{x}$ :

$$\|\tilde{x} - x_t\| = \|(x_t + \Delta tv_t^c/2) - x_t\| = \|\Delta tv_t^c/2\| = \Delta t/2\|v_t^c\|.$$

By assumption (A4),  $\|v_t^c\| \leq V_{\max}$ . Therefore:

$$\|\Delta v_{t-\Delta t/2}^\theta - \Delta v_t^\theta\| \leq L(\Delta tV_{\max}) = LV_{\max}\Delta t.$$

442 □

443 **A.3 Proof of Proposition 1**

**Proposition 2** (Bounded Single-Step Perturbation). *Let  $\hat{x}_{t-1}$  be the result of one Rectified-CFG++ step from  $x_t$ . Let  $\tilde{x}_{t-1} = x_t + \Delta tv_t^c(x_t)$  be the result of a pure conditional Euler step. Under assumption (A2), the deviation is:*

$$\|\hat{x}_{t-1} - \tilde{x}_{t-1}\| \leq \alpha(t)B\Delta t.$$

*Proof.* Using the definition of  $\hat{v}_{\lambda t}$  from Eq. (8):

$$\hat{x}_{t-1} = ODEStep(x_t, t, \hat{v}_{\lambda t}).$$

The pure conditional step is:

$$\tilde{x}_{t-1} = x_t + \Delta tv_t^c.$$

Subtracting these two equations:

$$\begin{aligned} \hat{x}_{t-1} - x_{t-1} &= (x_t + \Delta tv_t^c + \Delta t\alpha(t)\Delta v_{t-\Delta t/2}^\theta) - (x_t + \Delta tv_t^c) \\ \hat{x}_{t-1} - x_{t-1} &= \Delta t\alpha(t)\Delta v_{t-\Delta t/2}^\theta. \end{aligned}$$

Taking the norm:

$$\|\hat{x}_{t-1} - \tilde{x}_{t-1}\| = \|\Delta t\alpha(t)\Delta v_{t-\Delta t/2}^\theta\| = \Delta t\alpha(t)\|\Delta v_{t-\Delta t/2}^\theta\|.$$

By assumption (A2), the guidance direction magnitude is bounded by  $B$ . Hence,

$$\|\hat{x}_{t-1} - \tilde{x}_{t-1}\| \leq \Delta t\alpha(t)B.$$

444 □

445 **B Rectified-CFG++ Interpretation**

446 **B.1 Geometric intuition**

447 The overall Rectified-CFG++ displacement is a linear combination of already-trusted directions  
448 (conditional and unconditional)<sup>1</sup>. Hence the trajectory is “projected” onto the local tangent plane

<sup>1</sup>No orthogonal component of the form  $\eta \Delta v_t$  with a new  $\Delta v_t \notin T_{x_t} \mathcal{M}_t$  is introduced, in contrast to standard CFG when  $\omega > 1$ .



Figure 10: Samples produced by Flux-dev [1] using Rectified-CFG++.

449 at every step, preventing the dramatic colour saturation and structural distortions that may arise when  
 450 trajectories leave  $\mathcal{M}_t$  (Fig. 2). Rectified-CFG++ sampling method can be viewed geometrically as a  
 451 manifold-constrained trajectory refinement approach.

452 Rectified-CFG++ first performs a conditional predictor step, projecting the latent state onto the  
 453 learned manifold, then ensures that each intermediate representation remains manifold-aligned.  
 454 Subsequently, the adaptive corrector step applies a controlled, manifold-aware adjustment towards  
 455 the conditional trajectory. Geometrically (see Fig. 1), this two-step process ensures that trajectories  
 456 smoothly traverse along the manifold, allowing precise guidance towards text-conditioned regions  
 457 without manifold deviation or overshoot. Consequently, our method achieves both precise generation  
 458 aligned with the text conditions, and stable intermediate states that avoid drifting off-manifold (see  
 459 Fig. 3), significantly mitigating the artifacts typically induced by using CFG [13].

## 460 B.2 Enhanced Text Alignment and Manifold-Aware Generation

461 Rectified-CFG++ sampling achieves significantly improved text alignment by adaptively correcting  
 462 trajectories closer to the underlying learned data manifold. Traditional CFG approaches often push  
 463 generated images away from the natural manifold due to aggressive conditional updates, causing  
 464 unnatural distortions and poor aesthetics. Geometrically (see Fig. 1), this controlled navigation across  
 465 the latent space prevents manifold deviation, preserving intrinsic visual coherence and semantic  
 466 consistency. Consequently, our method delivers images that not only more precisely match textual  
 467 descriptions but also exhibit significantly enhanced quality, characterized by reduced visual artifacts,  
 468 greater perceptual realism, and smoother, more natural intermediate representations. Because the  
 469 update never strays far from  $\mathcal{M}_t$ , the model can faithfully realize additional conditional signals  
 470 (text prompts) without wasting capacity “returning” to the manifold. Empirically, this yields better  
 471 text-alignment and lower FID scores across guidance scales. Lemma A.1 explains that improvement  
 472 as a direct consequence of geometric consistency.

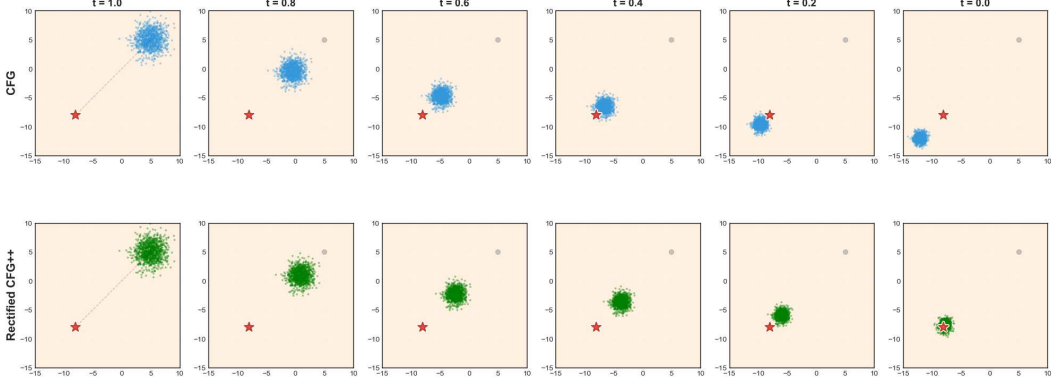


**Figure 11: Following [8], we show comparison of sampling trajectories under CFG (top row) and Rectified-CFG++ (bottom row).** Each column shows the evolution of 200 latent samples from  $t = 1.0$  to  $t = 0.0$  (left to right). *Markers:* the blue (top) and green (bottom) points trace the sample positions; the red star marks the target. Under standard CFG, the trajectories initially drift off the learned transport manifold—pulling sharply toward the conditional target only at later steps—resulting in abrupt, off-manifold jumps. In contrast, Rectified-CFG++ maintains a smooth, on-manifold path: the predictor step keeps samples close to the learned flow, and the corrector applies a controlled interpolation that steadily guides them toward the target.

### 473 B.3 Remark on guidance weights.

474 Throughout this paper we have described Rectified-CFG++ as a combination of unconditional and  
 475 conditional velocity fields with a time-dependent weight  $\alpha(t) \in \mathbb{R}_+$ :

$$\hat{v}_{\lambda,t} = v_t^c + \alpha(t)(v_{t-\frac{1}{2}}^c - v_{t-\frac{1}{2}}^u).$$

476 For many flow-matching models (e.g. Flux) we obtain best results when  $0 \leq \alpha(t) \leq 1$ , yielding a  
 477 true interpolation that keeps the trajectory firmly on-manifold. However, Rectified-CFG++ is not  
 478 restricted to  $\alpha(t) \leq 1$ . On models where the initial sampling steps are noticeably dependent on  
 479 conditional branches, we deliberately allowed  $\alpha(t) > 1$  during the early (high-noise) portion of the  
 480 trajectory, then decay it below 1 as  $t \rightarrow 0$ . The same predictor/corrector structure still applies; the  
 481 method merely chooses a schedule that can pass through both interpolation and mild extrapolation  
 482 regimes while remaining numerically stable. We therefore treat  $\alpha(t)$  as a time-scheduled re-weighting  
 483 rather than a strict convex coefficient:

$$\alpha(t) = \lambda_{\max}(1-t)^\gamma, \quad \lambda_{\max} \geq 0, \quad \gamma > 0 \quad (10)$$

484 with  $\lambda_{\max}$  tuned on a model basis. When  $\lambda_{\max} > 1$  the early steps behave like a soft extrapolation,  
 485 yet the empirical results in §4 show that the rectified predictor–corrector architecture still prevents  
 486 off-manifold divergences often observed when using naïve CFG.

---

#### Algorithm 2 RF sampling with CFG

---

**Require:** Trained Flux model  $v_\theta$ , text condition  $c$ , time steps  $N$ , step size  $\Delta t = 1/N$ .

```

1:  $x_1 \sim p_Z(z)$  ▷ Sample from noise distribution
2: for  $n = 0, 1, \dots, N-1$  do
3:    $t_n = n\Delta t$ 
4:    $\hat{v}_\theta \leftarrow (1-\omega)v_t^u + \omega v_t^c$ 
5:    $x_{t_{n-1}} \leftarrow x_{t_n} + \Delta t \hat{v}_\theta$  ▷ ODE
6: end for
7: return  $x_0$ 
```

---

## 487 C Related Work

### 488 C.1 Diffusion Models

489 Diffusion models (DMs) learn a stochastic (or deterministic) reverse process that gradually converts  
 490 Gaussian noise into natural images. Pioneering score-based work [37] and the DDPM formulation

Table 6: **Sampling update rules for various guidance strategies.** All methods operate in latent flow space using a velocity function  $v_\theta(z, t, \cdot)$ . Rectified-CFG++ introduces a predictor-corrector formulation combining unconditional drift and conditional correction.

Method	Velocity Functions Used	Update Equation
CFG	$v_\theta(z, t, y), v_\theta(z, t, \emptyset)$	$z_{t-1} = z_t + \Delta t \cdot [(1 - \omega) \cdot v_\theta(z_t, t, \emptyset) + \omega \cdot v_\theta(z_t, t, y)]$
APG	$v_\theta(z, t, y), \Delta v_t^{(\eta, r, \beta)}$	$z_{t-1} = z_t + \Delta t \cdot [v_\theta(z_t, t, y) + \Delta v_t^{(\eta, r, \beta)}]$
CFG-Zero*	$v_\theta(z, t, y), v_\theta(z, t, \emptyset)$	$z_{t+1} = z_t + \Delta t \cdot [(1 - \omega) \cdot s_t^* \cdot v_\theta(z_t, t, \emptyset) + \omega \cdot v_\theta(z_t, t, y)]$
Rect.-CFG++	$v_\theta(z, t, y), v_\theta(z, t, \emptyset)$	$z_{n+1} = z_n + \Delta t \cdot [v_\theta(z_n, t_n, y) + \alpha(t_n) \cdot (v_\theta(z_{n+\frac{\Delta}{2}}, t_n, y) - v_\theta(z_{n-\frac{\Delta}{2}}, t_n, \emptyset))]$

491 of [12] established the foundations that later enabled large-scale text-to-image systems such as  
492 GLIDE [25], DALLE [29], Imagen [34], and Stable Diffusion [30, 7]. Architectural innovations—e.g.  
493 latent-space diffusion [30] improved sample quality and inference speed.

## 494 C.2 Flow based Generative Models

495 Normalizing flows (NFs) parameterize an invertible transformation with a tractable Jacobian determinan-  
496 tant. Early discrete NFs (e.g. Glow [17]) were eclipsed by Continuous Normalizing Flows (CNFs)  
497 that solve an ODE defined by a neural velocity field [4, 9]. Recent flow-matching objectives cast  
498 generative modeling as learning a vector field that transports noise to data along a predefined sched-  
499 ule [21]. Rectified Flow (RF) [22] shows that a simple mean-squared objective suffices, eliminating  
500 simulation noise and yielding fast ODE solvers. In the text-to-image domain, model like SD3 [7],  
501 Lumina-Next [26], and FLUX [1] combine an RF objective with a large multi-modal diffusion  
502 transformer to deliver competitive image quality.

## 503 C.3 Guidance in Diffusion Models

504 Classifier guidance (CG) [6] injects gradients  
505 from an external classifier but demands a  
506 high-accuracy auxiliary network. Classifier-  
507 Free Guidance (CFG) [13] sidesteps this re-  
508 quirement by training conditional and un-  
509 conditional networks jointly and linearly extrapolat-  
510 ing their predictions during sampling. While  
511 CFG is now ubiquitous [25, 34, 29, 7], the  
512 high guidance scale pushes samples off the  
513 data manifold, causing over-saturation and  
514 structural collapse [5, 33]. Recent work re-  
515 places the single extrapolation with adaptive  
516 weighting or updates in sampler: Dynamic  
517 thresholding [34], CADS [32], ReCFG [41],  
518 characteristic-guidance [43], weight sched-  
519 ulers [39], Interval guidance [19], CFG++ [5],  
520 APG [33], AutoG [16], and step-limited  
521 CFG [19]. All are designed for stochastic dif-  
522 fusions; they either cannot be translated to flow  
523 based models, or underperform or destabilize  
524 the ODE trajectory [8].

525 CFG accumulates error over sampling steps, that  
526 scales with the norm of the unconditional velocity. These observations motivate our design of  
527 Rectified-CFG++: we reinterpret guidance as an interpolation in velocity-field space and embed  
528 it in an FM-compatible predictor–corrector ODE solver. By anchoring each predictor step with a  
529 conditional update to anchor the trajectory along the learned transport path and scheduling a purely  
530 interpolative corrector, we preserve the manifold geometry learned by the flow while still reaping  
531 the alignment gains of strong guidance. Extensive experiments show consistent improvements over  
532 vanilla CFG and its DM-centric variants across all flow based models.



Figure 12: Comparison of T2I results using Flux, with CFG, and with Rectified-CFG++.

533 **D Additional Experiments**

534 **D.1 Implementation Details**

535 All experiments were conducted on a single NVIDIA A100 40 GB GPU. Code was written in Python  
536 3.10, using PyTorch 2.0.1 and the latest HuggingFace Diffusers library. We evaluate four flow-based  
537 text-to-image backbones, taken from huggingface diffusers:

- 538 • **Stable Diffusion 3 [7] (SD3)** and **3.5 [7] (SD3.5)**: public weights from  
539 stabilityai/stable-diffusion-3-medium  
540 and stabilityai/stable-diffusion-3.5-large.
- 541 • **Flux-dev [1]**: guidance-distilled Flux models from black-forest-labs/FLUX.1-dev.
- 542 • **Lumina [26]**: public weights from Alpha-VLLM/Lumina-Image-2.0.

543 All models generate  $1024 \times 1024$  images from text prompts without additional fine-tuning.

544 **D.2 Details of User Study**

545 To assess perceptual quality and prompt fidelity, we conducted a blind four-way forced-choice  
546 comparison subjective study. No personally identifiable information was collected and standard  
547 guidelines for interacting with human subjects were followed. There was no risk incurred and no  
548 vulnerable population.

549 **Participants & Prompts:** We recruited 30 unique expert workers with knowledge of image  
550 processing, generative AI, computer vision, etc. Each worker was shown 32 distinct text prompts  
551 (e.g. “a number of people standing around a large group of luggage bags”), randomly sampled from  
552 our MS-COCO 10K [20] subset and Pick-a-Pic 1K [18].

553 **Interface & Instructions:** For each prompt, participants saw four generated images from a particu-  
554 lar T2I model - one per method (CFG [13], APG [33], CFG-Zero\* [8], and Rectified-CFG++) - in  
555 randomized order. The survey page (Fig. 13) instructed them to select the best image on four factors:

- 556 • **Detail:** fine structures and textures.
- 557 • **Naturalness & Color:** realism of scene and color consistency.
- 558 • **Text Legibility:** clarity of any embedded text or signage.
- 559 • **Overall:** overall holistic preference.

560 Participants were encouraged to switch to a larger screen or zoom if necessary to inspect fine details.  
561 We repeated this for all four T2I models, i.e. SD3/3.5 [7], Lumina 2.0 [26], and Flux [1].

562 **Data Collection:** Each (prompt, generations) pair was rated by 30 independent expert participants,  
563 yielding 15360 total responses across all four T2I models. Image positions and prompt order were  
564 fully randomized to mitigate presentation bias.

565 We aggregate per-pair preferences for each method, the fraction of times it was chosen as best.  
566 As shown in Fig. 8, Rectified-CFG++ is preferred over all alternatives on Detail, Naturalness &  
567 Color, Text Legibility, and Overall confirming its advantages in fine detail, color fidelity, and prompt  
568 adherence.

569 **D.3 More Quantitative Results**

570 Here, we report further metric-based comparisons of Rectified-CFG++ across multiple datasets,  
571 models, guidance scales, and sampling budgets.

572 **LAION-Aesthetic and Pick-a-Pic Evaluations:** Table 7 summarizes performance on the LAION-  
573 Aesthetic 1K subset. Rectified-CFG++ consistently lowers FID and improves CLIP-Score, ImageRe-  
574 ward, PickScore and HPSv2 across all four backbones. For example, on Flux-dev the FID drops  
575 from 120.13 to 112.19, while ImageReward jumps from 0.0968 to 0.6849. Table 8 presents results

Welcome! Thank you for your help in improving the next generation of text-to-image models.

You will see now 32 sets of images in total. Please select your preference for the best image out of the displayed images.

Overall, you may consider the following factors: image detail, realism of scene, color naturalness and consistency, prompt alignment, and text fidelity. Pay special attention to artifacts like malformed hands or limbs, misshaped objects, and so on.

Please switch to a larger screen/zoom to observe details if you find providing ratings is difficult.

The interface consists of several sections:

- Top:** A large text area with instructions, followed by a red "next" button.
- Text Prompt:** "the men play soccer on the beach with no shoes".
- Image Grid:** Four small images labeled 1, 2, 3, and 4, showing men playing soccer on a beach.
- Rating Scales:**
  - Detail:** Buttons for 1, 2, 3, 4.
  - Naturalness and color:** Buttons for 1, 2, 3, 4.
  - Text legibility:** Buttons for 1, 2, 3, 4.
  - Overall:** Buttons for 1, 2, 3, 4.
- Bottom Left:** A text box containing instructions for selecting the best image based on the provided factors.

**Figure 13: Interface for the user study.** Top: participants first read detailed instructions on the evaluation criteria (detail, naturalness & color, text legibility, overall) and usage guidelines (e.g. zooming, screen size). Bottom left: an example text prompt together with the four generated images shown in randomized order. Bottom right: the corresponding multiple-choice rating options for each criterion, where workers select which of the four images best satisfies the given factor.

576 on the Pick-a-Pic 1K prompts. Rectified-CFG++ yields uniformly higher CLIP-Score, Aesthetic,  
577 ImageReward, PickScore and HPSv2.

578 **Guidance Scale Ablations:** Table 9 reports FID, CLIP and ImageReward for Flux-dev [1] under six  
579 different guidance scales ( $\omega, \lambda$ ). Across all settings—from mild to aggressive guidance—Rectified-  
580 CFG++ matches or exceeds CFG, with best results highlighted in orange. Table 10 extends this  
581 multi-scale comparison to SD3 [7] and SD3.5 [7] on both MS-COCO-1K and LAION-Aesthetic-1K.

582 **Sampling Step Ablations:** Finally, Tables 11, 12 and 13 compare standard CFG and Rectified-  
583 CFG++ as the number of function evaluations (NFEs) varies from 5 to 60. Even with as few as 5  
584 NFEs, Rectified-CFG++ reduces Flux [1]’s FID from 177.8 to 71.2 and boosts ImageReward by over  
585 2.4 points. Similar gains are observed on SD3 [7] and SD3.5 [7]: at 15 NFEs, SD3’s FID falls from  
586 72.7 to 69.1, and at 28 NFEs SD3.5’s ImageReward rises from 0.72 to 0.77. These results confirm  
587 that Rectified-CFG++ not only improves ultimate quality but also accelerates convergence under  
588 limited sampling budgets.

#### 589 D.4 More Qualitative Results

590 To complement our quantitative evaluation, we present extensive qualitative evaluations across four  
591 state-of-the-art flow-based text-to-image backbones (SD3 [7], SD3.5 [7], Flux-dev [1], and Lumina  
592 2.0 [26]). In each case we select diverse, challenging prompts—ranging from signage and typography  
593 to fantasy scenes, and text-heavy compositions—and show side-by-side renderings in Figures 14–18.

594 **Improved Prompt Fidelity and Detail:** Across all models, Rectified-CFG++ better captures the  
595 precise wording, style, and layout of complex text prompts. In Figure 14 (top) the “Welcome to  
596 Dustvale” billboard exhibits crisp, correctly proportioned lettering under Rectified-CFG++, whereas  
597 CFG renders unclear and distant characters. Similarly, for the “Elixir of Time” grimoire (Figure 14),  
598 our method preserves fine runic serifs and balanced illumination, avoiding the blotchy over-saturation  
599 and gibberish text seen with CFG.

600 **Enhanced Geometry and Color Balance:** Rectified-CFG++ produces more coherent object shapes  
601 and natural color distributions. In the ruined observatory prompt (Figure 14, middle left), the dome  
602 geometry remains intact and the night-sky hues appear smoothly graded, in contrast to the heavy  
603 color clipping and warped glass panes under CFG.

604 **Robustness on Artistic and Text-Intensive Tasks:** In text-heavy or highly stylized contexts  
605 (Figures 19–20), CFG often fails to form legible letters or distorts ornamented scripts, whereas  
606 Rectified-CFG++ maintains semantic clarity and faithful adherence to prompt instructions. For  
607 example, the medieval scroll (“Quest Accepted”) and the glowing “IGNIS SCRIPTUM” spell circle  
608 are rendered with sharp, even strokes only under our method.

609 **Stable Intermediate Trajectories:** Figure 21 visualizes successive denoised latents for two prompts  
610 using both CFG and Rectified-CFG++. While CFG trajectories diverge off-manifold—yielding over-  
611 saturated patches and incoherent forms in early timesteps, Rectified-CFG++ remains tightly clustered,  
612 preserving anatomical and geometric consistency at every step. Even with only 7 NFEs (Figure 22),  
613 our sampler produces high-fidelity results far sooner, demonstrating accelerated convergence.

614 **Generalization Across Models:** Figures 16, 17 and 18 confirm that these qualitative gains extend  
615 across all flow-based models tested - SD3 [7], SD3.5 [7], Flux-dev [1], and Lumina 2.0 [26]. Whether  
616 generating playful scenes (“a cat in a space suit skiing”), hyper-realistic product shots (“leaf-covered  
617 Porsche”), or fantastical landscapes (floating island cities, glowing jellyfish cathedrals), Rectified-  
618 CFG++ consistently yields crisper details, fewer artifacts, and stronger alignment to both text and  
619 style cues.

620 Together, these qualitative examples illustrate that the manifold-aware update of Rectified-CFG++  
621 not only improves objective metrics but also delivers visibly superior images in a wide variety of  
622 challenging text-to-image scenarios.

## 623 E Failure Cases and Limitations

624 Although Rectified-CFG++ greatly reduces off-manifold artifacts, we observe that, for prompts  
 625 requiring multiple interacting objects the method sometimes misplaces secondary elements or fails to  
 626 respect relative scale. On further investigation, we observe that these limitations arise from underlying  
 627 T2I model, and is consistent across all guidance methods. Our approach, being entirely training-free,  
 628 inherits the dependence on pretrained velocity accuracy, any systematic bias or normal-space drift in  
 629  $v_\theta$  may propagate through Rectified-CFG++.

## 630 F Ethics Statement

631 Given the rapid progress of generative models, it has become easier than ever to produce convincing—  
 632 but potentially misleading—synthetic content. Although such tools unlock new efficiencies  
 633 and creative avenues, they also raise important ethical challenges. Readers interested in a deeper  
 634 treatment of these issues are referred to the discussion in [31].

## 635 G Broader Impact Statement

636 **Social impact:** Image generation with flow-based models potentially has both positive and negative  
 637 social impact. This method provides a handy tool to the general public for generating a wide variety  
 638 of images which can help visualize their artistic ideas. On the other hand, our work on improving  
 639 sampling quality in these models poses a risk of generating art that closely mimics or infringes upon  
 640 existing copyrighted material, leading to legal and ethical issues. More broadly, our method inherits  
 641 the risks from T2I models which are capable of generating fake content that can be misused by  
 642 malicious users.

643 **Safeguards:** This work builds upon the official implementations and pre-trained weights of the  
 644 foundation models referenced in the main text. These methods along with the diffusers library has  
 645 a mechanism to filter offensive image generations. Our method Rectified-CFG++ inherits these  
 646 safeguards.

647 **Reproducibility:** Apart from the pseudocode and implementation details provided in the paper, the  
 648 source code is available on the project page: <https://rectified-cfgpp.github.io/>.

Table 7: Quantitative evaluation of Rectified-CFG++ across T2I models on LAION-Aesthetic 1K samples. Best values highlighted in orange, second-best in gray.

Model	Guidance	FID ↓	CLIP ↑	Aesthetic ↑	ImageReward ↑	PickScore ↑	HPSv2 ↑
Lumina [26]	CFG	112.3344	0.2717	5.6823	0.4173	0.5913	0.2324
	Rect. CFG++ (Ours)	<b>110.4973</b>	<b>0.2771</b>	<b>5.6823</b>	<b>0.4108</b>	<b>0.4087</b>	<b>0.2098</b>
SD3 [7]	CFG	107.2530	0.3092	6.0328	0.5800	0.4708	0.2464
	Rect. CFG++ (Ours)	<b>105.9037</b>	<b>0.3125</b>	<b>5.9750</b>	<b>0.6840</b>	<b>0.5292</b>	<b>0.2549</b>
SD3.5 [7]	CFG	108.4751	0.3162	6.1245	0.6984	0.4798	0.2543
	Rect. CFG++ (Ours)	<b>107.3915</b>	<b>0.3164</b>	<b>5.9528</b>	<b>0.7635</b>	<b>0.5202</b>	<b>0.2569</b>
Flux-dev [1]	CFG	120.1258	0.2939	4.8033	0.0968	0.3469	0.2181
	Rect. CFG++ (Ours)	<b>112.1902</b>	<b>0.3065</b>	<b>5.5694</b>	<b>0.6849</b>	<b>0.6531</b>	<b>0.2518</b>

Table 8: Quantitative Evaluation of Rectified-CFG++ Across T2I Models on Pick-a-Pic 1K samples. Best values highlighted in orange, second-best in gray.

Model	Guidance	CLIP $\uparrow$	Aesthetic $\uparrow$	ImageReward $\uparrow$	PickScore $\uparrow$	HPSv2 $\uparrow$
Lumina [26]	CFG	0.3336	5.6996	1.0080	0.5841	0.2910
	Rect. CFG++ (Ours)	<b>0.3378</b>	<b>5.8770</b>	<b>0.7621</b>	<b>0.4159</b>	<b>0.2982</b>
SD3 [7]	CFG	0.3453	5.7286	0.8268	0.4908	0.2859
	Rect. CFG++ (Ours)	<b>0.3487</b>	<b>5.6441</b>	<b>0.9364</b>	<b>0.5092</b>	<b>0.2933</b>
SD3.5 [7]	CFG	0.3551	6.0411	1.0181	0.5211	0.2980
	Rect. CFG++ (Ours)	<b>0.3564</b>	<b>6.8767</b>	<b>1.0267</b>	<b>0.4789</b>	<b>0.2996</b>
Flux-dev [1]	CFG	0.3312	5.1419	0.5336	0.3428	0.2609
	Rect. CFG++ (Ours)	<b>0.3406</b>	<b>5.8455</b>	<b>0.9641</b>	<b>0.6572</b>	<b>0.2974</b>

Table 9: Multi-scale quantitative evaluation of the Flux [1] model (28 NFEs) on MS-COCO 1K and LAION-Aesthetics 1K. We implemented Flux [1] using both standard CFG [13] and Rectified-CFG++ as the guidance scales ( $\omega, \lambda$ ) were varied. Lower ( $\downarrow$ ) FID and higher ( $\uparrow$ ) CLIP and ImageReward scores indicate better performance. Best values highlighted in orange, second-best in gray. (Best viewed zoomed in.)

Method	$\omega = 1.5, \lambda = 0.2$			$\omega = 3.0, \lambda = 0.3$			$\omega = 3.5, \lambda = 0.5$			$\omega = 4.0, \lambda = 0.7$			$\omega = 6.0, \lambda = 1.0$			$\omega = 10.0, \lambda = 1.2$		
	FID $\downarrow$	CLIP $\uparrow$	ImgRwd $\uparrow$	FID $\downarrow$	CLIP $\uparrow$	ImgRwd $\uparrow$	FID $\downarrow$	CLIP $\uparrow$	ImgRwd $\uparrow$	FID $\downarrow$	CLIP $\uparrow$	ImgRwd $\uparrow$	FID $\downarrow$	CLIP $\uparrow$	ImgRwd $\uparrow$	FID $\downarrow$	CLIP $\uparrow$	ImgRwd $\uparrow$
<b>MS-COCO 1K</b>																		
CFG	73.7315	0.3451	0.9973	85.1933	0.3283	0.4762	96.3729	0.3147	0.1467	105.9574	0.3052	-0.1258	130.1050	0.2694	-0.8706	146.9677	0.2363	-1.4388
Rect-CFG++	<b>74.2674</b>	<b>0.3445</b>	<b>1.0022</b>	<b>74.6668</b>	<b>0.3449</b>	<b>1.0030</b>	<b>75.6161</b>	<b>0.3446</b>	<b>1.0248</b>	<b>75.3240</b>	<b>0.3462</b>	<b>1.0274</b>	<b>75.4086</b>	<b>0.3462</b>	<b>1.0241</b>	<b>76.1754</b>	<b>0.3462</b>	<b>1.0434</b>
<b>LAION-Aesthetic 1K</b>																		
CFG	68.8747	0.3061	0.6808	72.4575	0.3006	0.3201	85.4752	0.2856	-0.1378	96.2533	0.2707	-0.5708	107.0080	0.2518	-0.9278	131.8580	0.2183	-1.4793
Rect-CFG++	<b>69.4215</b>	<b>0.3023</b>	<b>0.6844</b>	<b>69.1240</b>	<b>0.3054</b>	<b>0.7091</b>	<b>68.7578</b>	<b>0.3072</b>	<b>0.7033</b>	<b>68.3281</b>	<b>0.3094</b>	<b>0.7281</b>	<b>68.4089</b>	<b>0.3092</b>	<b>0.7396</b>	<b>68.3509</b>	<b>0.3103</b>	<b>0.7356</b>

Table 10: Multi-scale quantitative evaluation of the SD3 [7] and SD3.5 [7] T2I models using CFG and Rectified-CFG++ (28 NFEs) on the MS-COCO 1K and LAION-Aesthetic 1K datasets, as the guidance scales ( $\omega, \lambda$ ) were varied. Lower FID and higher CLIP ImageReward indicate better performance. (Best viewed zoomed in.)

Model	Guidance	$\omega = 2.0, \lambda = 2.0$			$\omega = 3.0, \lambda = 3.5$			$\omega = 3.5, \lambda = 5.0$			$\omega = 4.5, \lambda = 7.0$			$\omega = 6.0, \lambda = 9.0$			$\omega = 10.0, \lambda = 12.0$		
		FID $\downarrow$	CLIP $\uparrow$	ImgRwd $\uparrow$	FID $\downarrow$	CLIP $\uparrow$	ImgRwd $\uparrow$	FID $\downarrow$	CLIP $\uparrow$	ImgRwd $\uparrow$	FID $\downarrow$	CLIP $\uparrow$	ImgRwd $\uparrow$	FID $\downarrow$	CLIP $\uparrow$	ImgRwd $\uparrow$	FID $\downarrow$	CLIP $\uparrow$	ImgRwd $\uparrow$
<b>MS-COCO 1K</b>																			
SD3	65.6608	0.3407	0.6658	68.5913	0.3469	0.9180	69.5383	0.3486	1.0035	70.4443	0.3491	1.0162	69.8652	0.3477	1.0292	70.4416	0.3432	0.9015	
Rect-CFG++	<b>66.6997</b>	<b>0.3456</b>	<b>0.9037</b>	<b>67.7332</b>	<b>0.3467</b>	<b>0.9739</b>	<b>67.7651</b>	<b>0.3463</b>	<b>0.9838</b>	<b>68.7935</b>	<b>0.3476</b>	<b>1.0152</b>	<b>68.9262</b>	<b>0.3475</b>	<b>1.0067</b>	<b>69.7212</b>	<b>0.3394</b>	<b>0.7768</b>	
SD3.5	66.9723	0.3468	0.9239	67.7133	0.3515	1.0530	67.9481	0.3518	0.9584	68.2184	0.3509	1.0522	69.0347	0.3476	0.9633	74.7053	0.3388	0.7214	
Rect-CFG++	<b>67.3784</b>	<b>0.3506</b>	<b>1.0140</b>	<b>67.8372</b>	<b>0.3505</b>	<b>1.0558</b>	<b>67.1495</b>	<b>0.3506</b>	<b>1.0845</b>	<b>66.4993</b>	<b>0.3509</b>	<b>1.0807</b>	<b>67.3128</b>	<b>0.3481</b>	<b>0.9884</b>	<b>76.2934</b>	<b>0.3340</b>	<b>0.5523</b>	
<b>LAION-Aesthetic 1K</b>																			
SD3	109.6643	0.3025	0.3825	107.2510	0.3005	0.5800	105.1719	0.3131	0.7125	106.4279	0.3135	0.7055	105.1566	0.3110	0.6641	105.5225	0.3018	0.4775	
Rect-CFG++	<b>109.0101</b>	<b>0.3103</b>	<b>0.6019</b>	<b>107.4210</b>	<b>0.3129</b>	<b>0.6655</b>	<b>105.6636</b>	<b>0.3119</b>	<b>0.6784</b>	<b>105.9037</b>	<b>0.3125</b>	<b>0.6840</b>	<b>104.8691</b>	<b>0.3129</b>	<b>0.7278</b>	<b>105.7928</b>	<b>0.2986</b>	<b>0.3902</b>	
CFG	112.6539	0.3075	0.5507	108.4751	0.3162	0.6984	107.1446	0.3183	0.7675	105.8216	0.3173	0.7302	107.1061	0.3122	0.6257	111.3334	0.2955	0.2583	
Rectified-CFG++	<b>110.2739</b>	<b>0.3155</b>	<b>0.7149</b>	<b>107.3088</b>	<b>0.3178</b>	<b>0.7440</b>	<b>107.7859</b>	<b>0.3174</b>	<b>0.7867</b>	<b>107.3915</b>	<b>0.3164</b>	<b>0.7623</b>	<b>106.6539</b>	<b>0.3140</b>	<b>0.6757</b>	<b>112.0855</b>	<b>0.2916</b>	<b>0.1052</b>	

Table 11: Evaluation of the Flux [1] model across different sampling steps (NFEs) on MS-COCO 1K. We compare standard CFG and Rectified CFG++ across key metrics. Lower FID and higher CLIP/ImageReward indicate better performance.

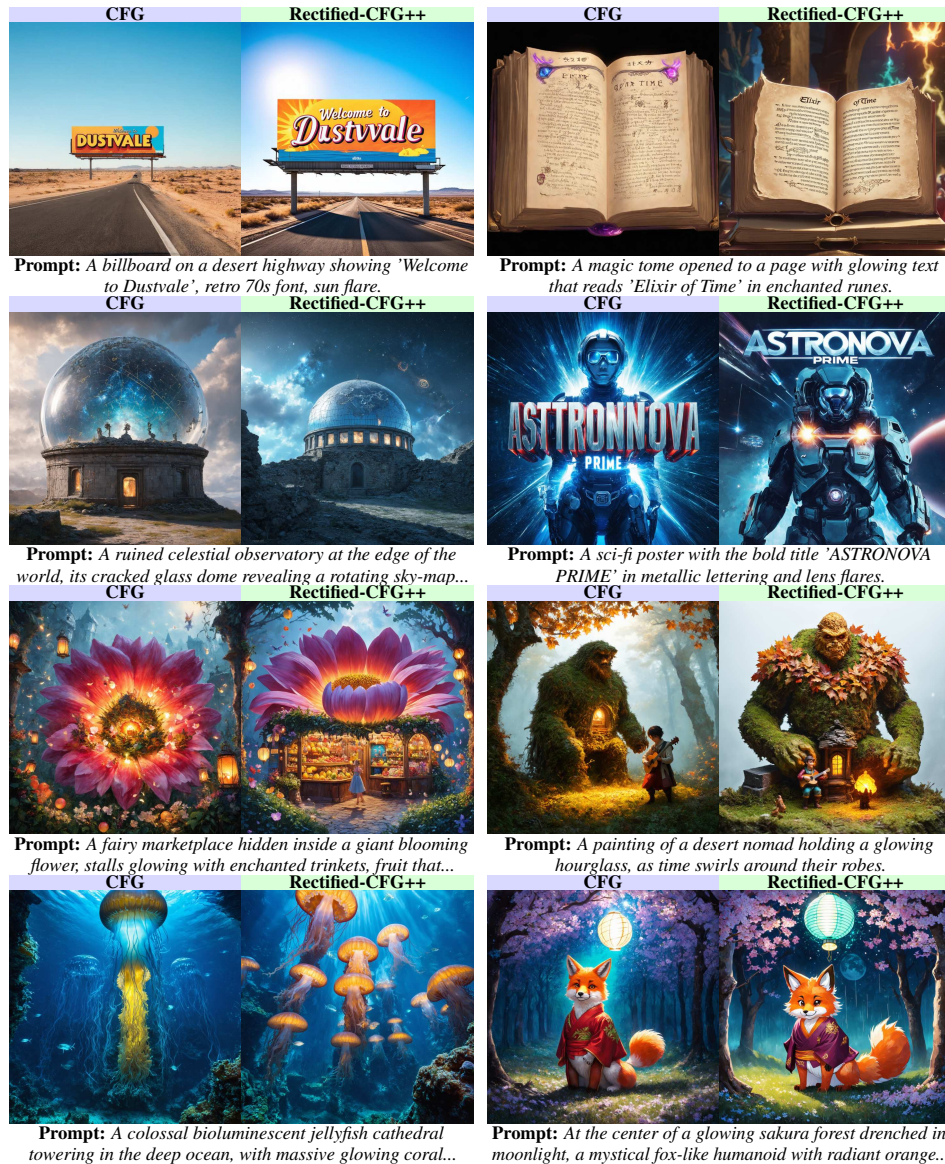
Steps	FID $\downarrow$		CLIP $\uparrow$		ImageReward $\uparrow$	
	CFG	Rect.-CFG++	CFG	Rect.-CFG++	CFG	Rect.-CFG++
5	177.81	<b>71.17</b>	0.24	<b>0.33</b>	-1.54	<b>0.93</b>
15	114.94	<b>74.47</b>	0.30	<b>0.34</b>	-0.38	<b>1.04</b>
28	85.82	<b>75.34</b>	0.32	<b>0.34</b>	0.46	<b>1.01</b>
40	78.47	<b>74.13</b>	0.34	<b>0.35</b>	0.80	<b>1.04</b>
50	76.88	<b>75.17</b>	0.34	<b>0.35</b>	0.92	<b>1.01</b>
60	85.82	<b>75.34</b>	0.32	<b>0.34</b>	0.47	<b>1.02</b>

Table 12: Evaluation of the SD3 [7] model across different sampling steps (NFEs) on MS-COCO 1K. Comparison between standard CFG and Rectified-CFG++.

Steps	FID $\downarrow$		CLIP $\uparrow$		ImageReward $\uparrow$	
	CFG	Rect. CFG++	CFG	Rect. CFG++	CFG	Rect. CFG++
5	129.0333	<b>112.8318</b>	0.2654	<b>0.2779</b>	-1.4232	<b>-1.0803</b>
15	72.7270	<b>69.0608</b>	0.3427	<b>0.3418</b>	0.6826	<b>0.7326</b>
28	72.7399	<b>70.0272</b>	0.3461	<b>0.3432</b>	0.8961	<b>0.8294</b>
40	72.8198	<b>68.7318</b>	0.3449	<b>0.3453</b>	0.9244	<b>0.8836</b>
50	73.4710	<b>70.1959</b>	0.3456	<b>0.3463</b>	0.9244	<b>0.8710</b>
60	73.2599	<b>68.9540</b>	0.3450	<b>0.3456</b>	0.9143	<b>0.8986</b>

Table 13: Evaluation of the SD3.5 [7] model across different sampling steps (NFEs) on MS-COCO 1K. Comparison between standard CFG and Rectified-CFG++.

Steps	FID ↓		CLIP ↑		ImageReward ↑	
	CFG	Rect. CFG++	CFG	Rect. CFG++	CFG	Rect. CFG++
5	85.9537	<b>149.3422</b>	0.3214	<b>0.2300</b>	-0.1806	<b>-1.5413</b>
15	69.4994	<b>69.3713</b>	0.3361	<b>0.3430</b>	0.6813	<b>0.6820</b>
28	69.8250	<b>69.1095</b>	0.3435	<b>0.3443</b>	0.7274	<b>0.7750</b>
40	69.2999	<b>69.2601</b>	0.3431	<b>0.3437</b>	0.7310	<b>0.7708</b>
50	69.3650	<b>69.0434</b>	0.3452	<b>0.3443</b>	0.7506	<b>0.7705</b>
60	68.8897	<b>67.9782</b>	0.3438	<b>0.3441</b>	0.7348	<b>0.7611</b>



**Figure 14: Outcome of the SD3 [7] T2I models when using CFG vs Rectified-CFG++ for a variety of prompts.** Our method consistently improves image generation quality by producing more coherent, semantically aligned, and visually rich results, even under complex or artistic prompting scenarios.

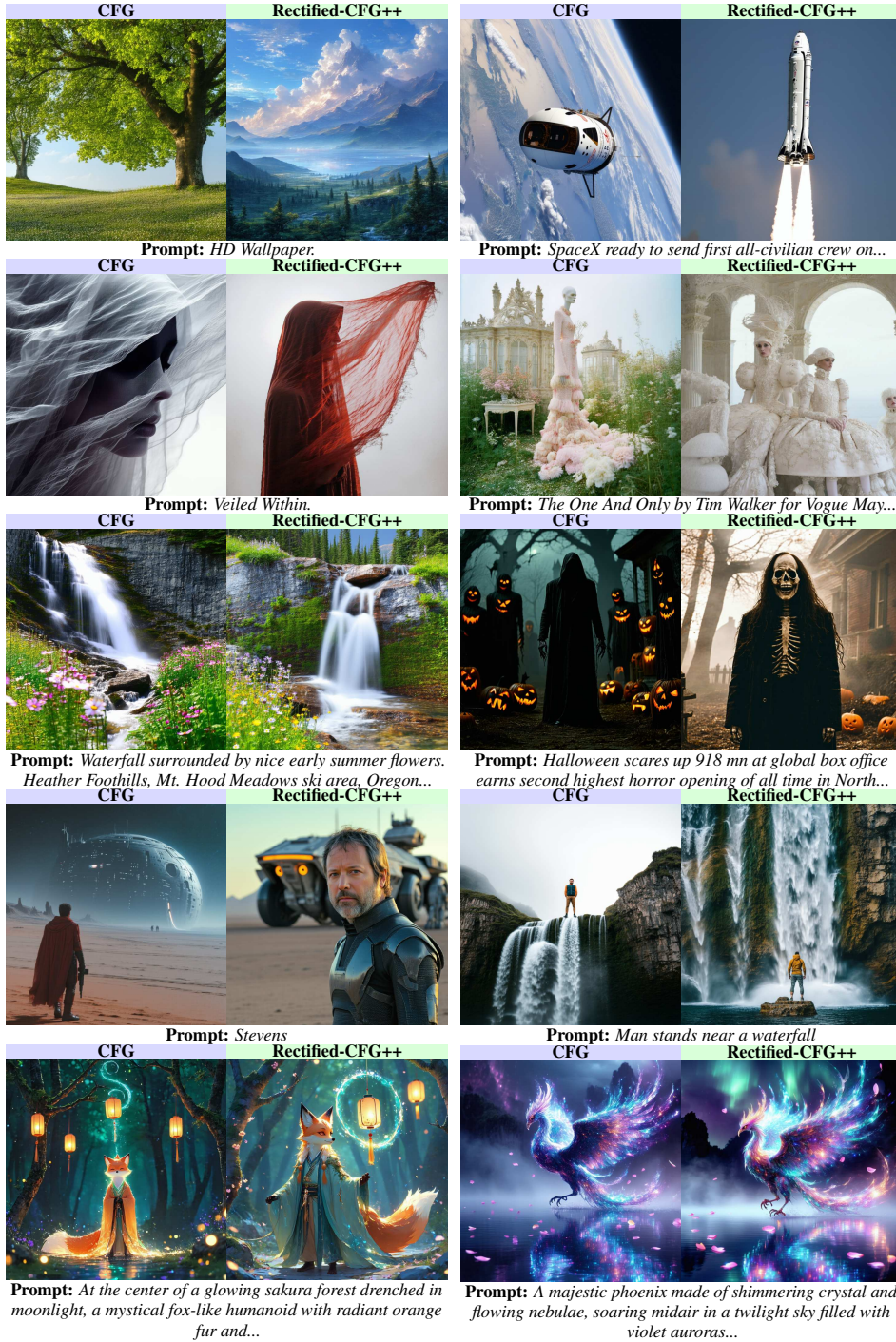


Figure 15: Outcome of SD3.5 [7] when using CFG vs Rectified-CFG++ for a variety text prompts.

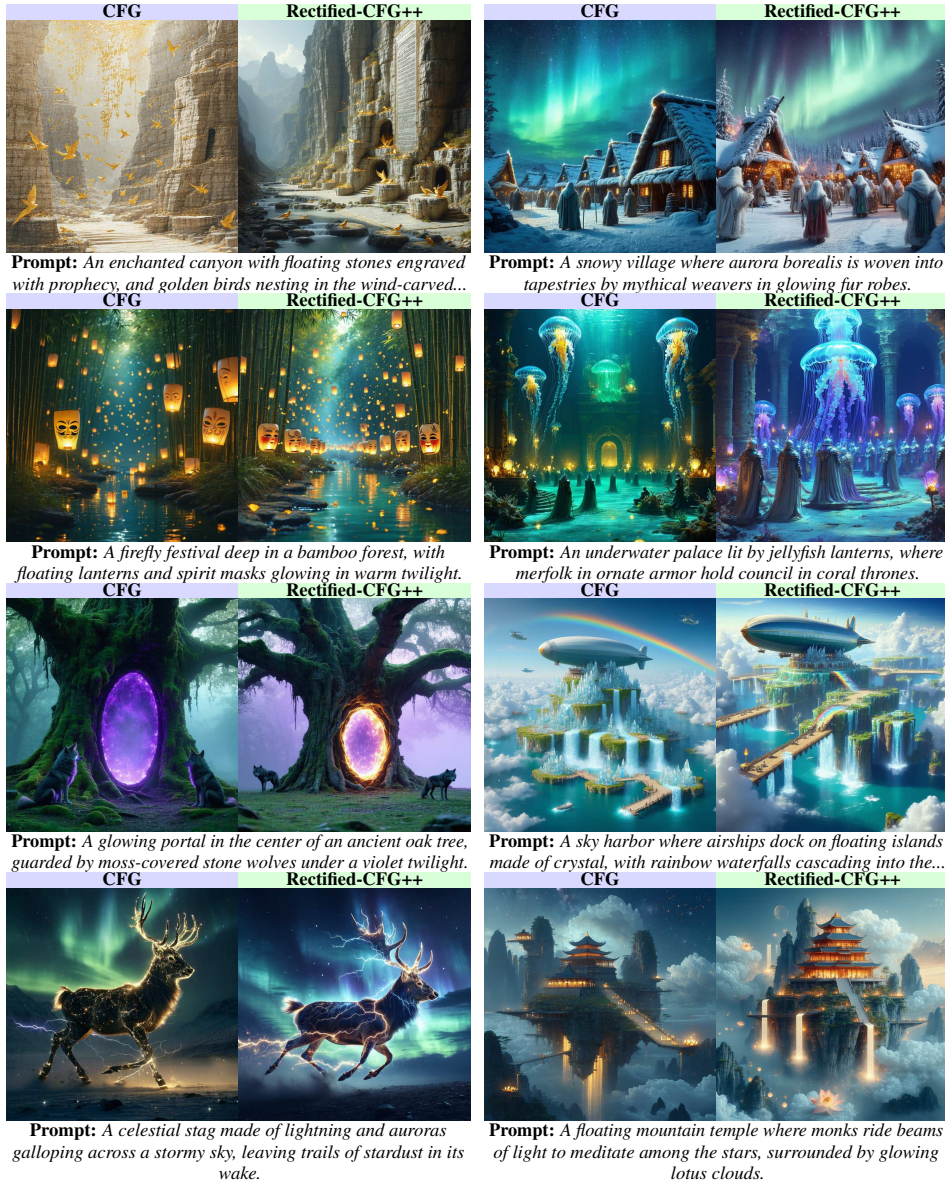


Figure 16: More examples for SD3.5 [7] with CFG vs Rectified-CFG++ for a variety of text prompts.

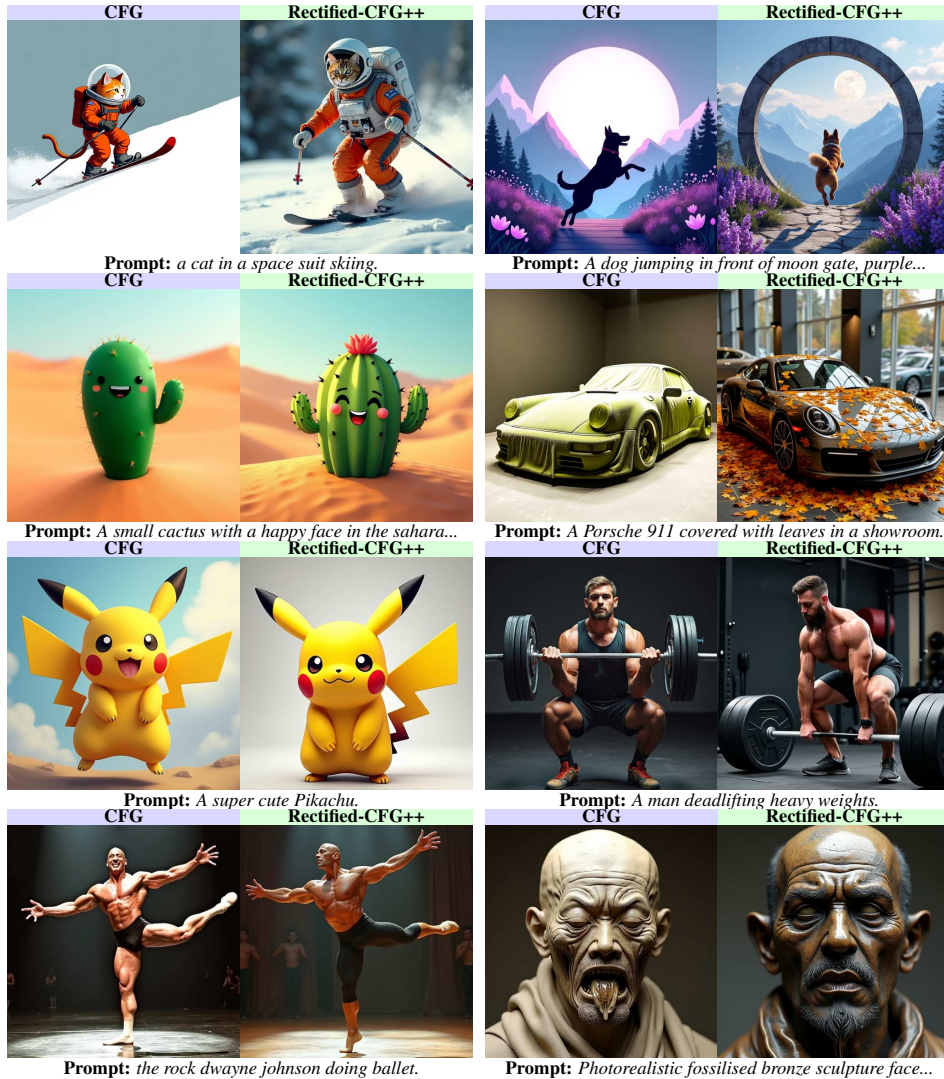


Figure 17: Outcome of Flux [1] with CFG vs Rectified-CFG++ for a variety of text prompts.

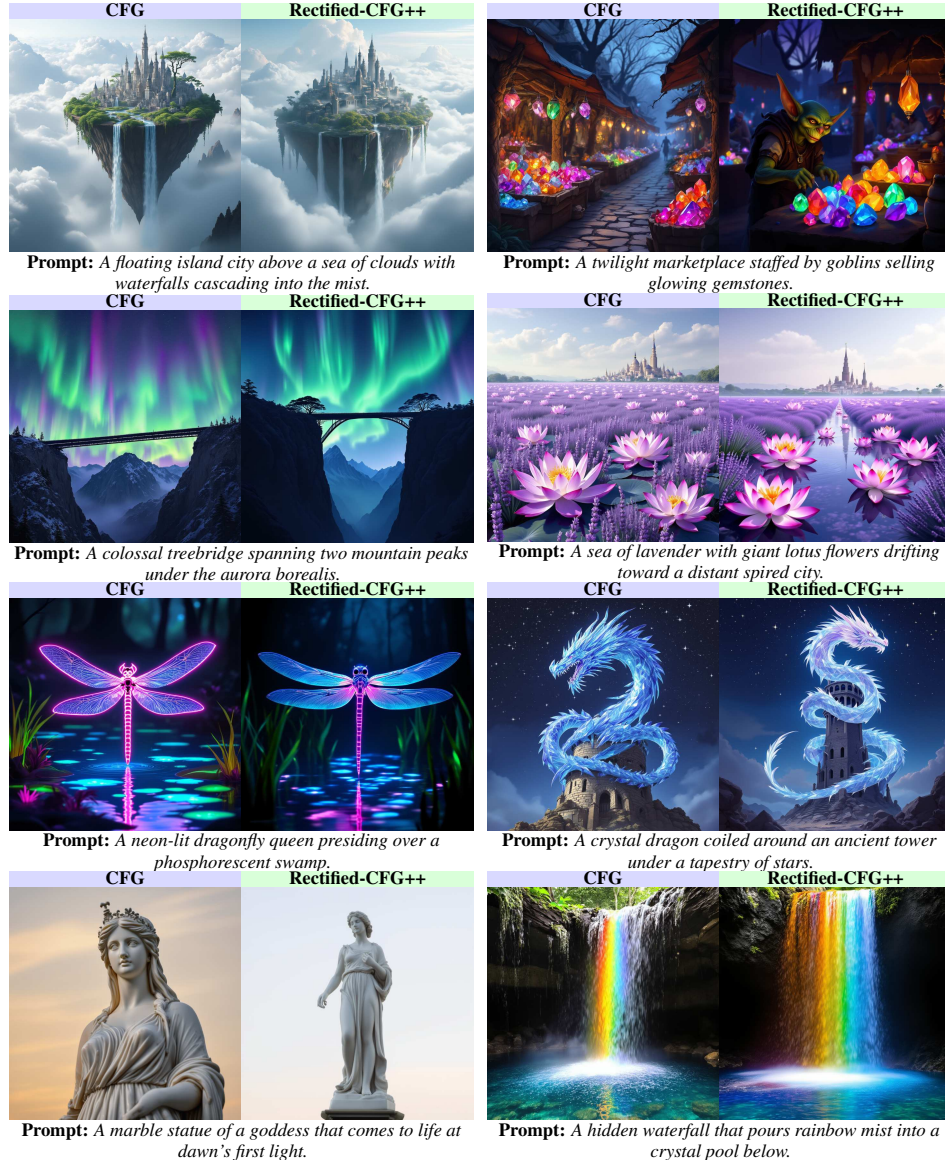


Figure 18: **Outcome of Lumina [26] with CFG vs Rectified-CFG++ for a variety of text prompts.** Rectified-CFG++ improves compositional clarity, color balance, and prompt adherence under fantastical and artistic conditions.



**Prompt:** A medieval scroll displaying the phrase “Quest Accepted” in ornate gothic script.

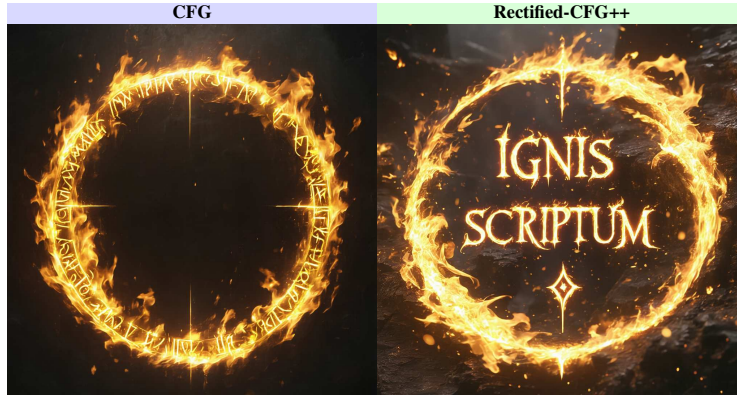


**Prompt:** A giant, ancient coin partially buried in snow, engraved with ‘DOMINION ETERNAL’ around its rim.



**Prompt:** A magical contract floating in midair, the clause ‘SOULBOUND BY NIGHTFALL’ glowing in arcane script.

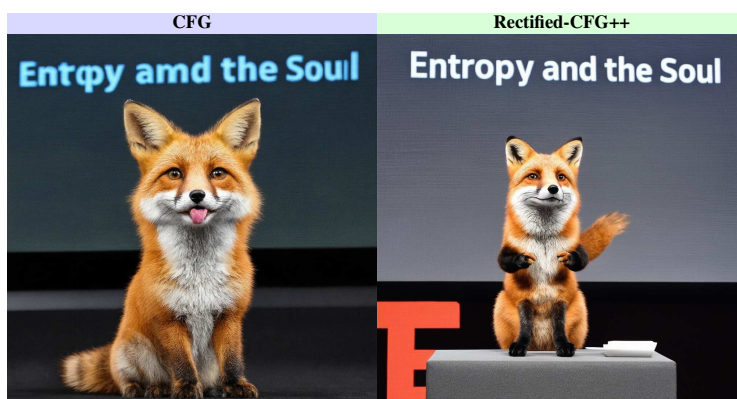
**Figure 19: Comparison of text generation using CFG against Rectified-CFG++ in the SD3.5 [7] (Part 1).** Rectified-CFG++ improves legibility and semantic preservation, especially in stylized or aged contexts.



**Prompt:** A golden spellcircle inscribed with the phrase 'IGNIS SCRIPTUM' in liquid fire-gold runes, hovering midair.



**Prompt:** A lizard monk painting 'Breathe, Don't Bite' in perfect cursive on rice paper with a brush.



**Prompt:** A fox giving a TED talk titled 'Entropy and the Soul' written on a digital board behind.

Figure 20: Comparison of text generation using CFG against Rectified-CFG++ in the SD3 [7] (Part 2). Even in highly decorative or weathered lettering styles, Rectified-CFG++ retains better visual clarity and accurate text composition.

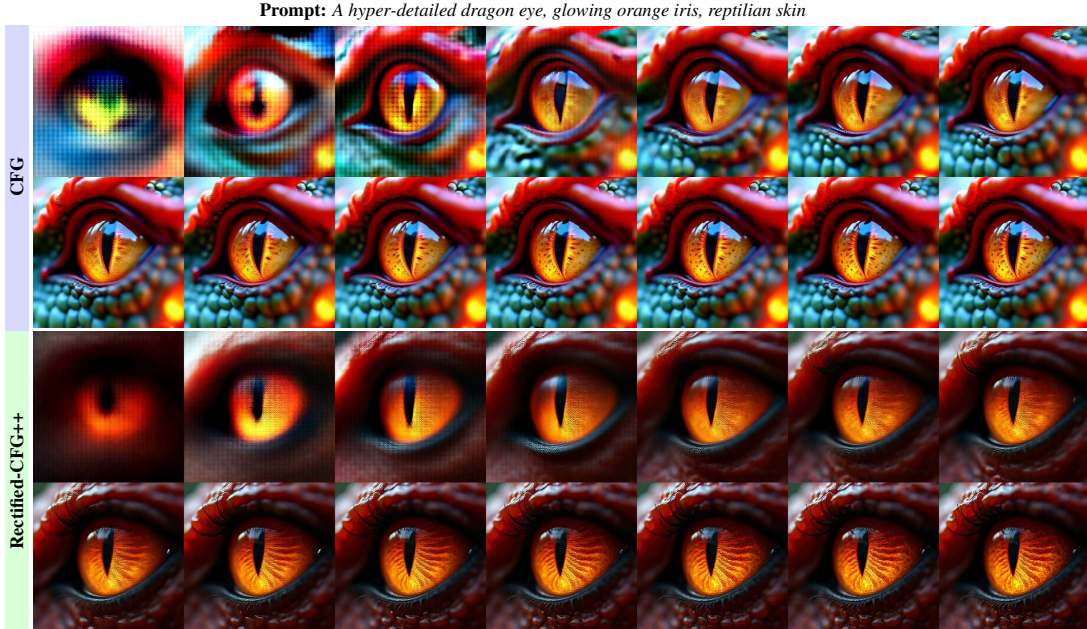
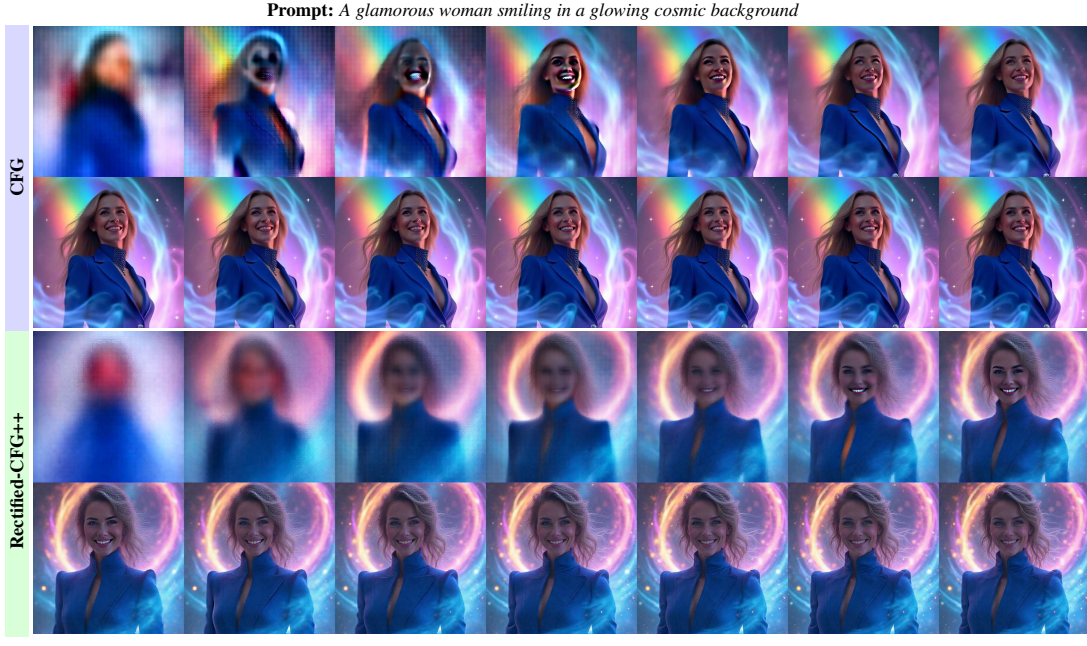


Figure 21: **Intermediate timestep visualizations of CFG and Rectified-CFG++.** Progressive decoding of denoised latents across intermediate timesteps using CFG (top row) and Rectified-CFG++ (bottom row). For each prompt, we used total of 14 sampling steps, progressing from  $t = 1000$  (top left) to  $t = 0$  (bottom right). While CFG suffers from unstable off-manifold transitions early on, resulting in oversaturated colors and incoherent forms, Rectified-CFG++ maintained consistent, semantically grounded updates throughout. This enables significantly improved anatomical realism, color harmony, and overall fidelity under a reduced lesser computational budget.

**Prompt:** A highly detailed sculpture of a dog made entirely of reflective molten gold, mid-jump, with fluid metallic textures and dynamic lighting.



**Prompt:** A celestial lion composed of stardust and translucent sapphire, resting atop a glowing moonrock pedestal under a swirling galaxy sky..



**Prompt:** At the center of a glowing sakura forest drenched in moonlight, a mystical fox-like humanoid with radiant orange fur and nine shimmering tails stands guarding...



**Prompt:** Inside a ruined cathedral overtaken by vines and time, a mechanical artisan — half-human, half-clockwork — adjusts a floating, glowing time orb...



Figure 22: **7-step sampling comparison between CFG and Rectified-CFG++.** Each pair of rows shows intermediate denoised and decoded latents for all 7 sampling steps. Rectified-CFG++ consistently delivered better generated outcomes even in the early time steps while keeping the overall generation process on-manifold.

Table 14: Comprehensive list of prompts used across figures, experiments, and qualitative evaluations in the paper.

ID	Prompt
1	A majestic phoenix made of shimmering crystal and flowing nebulae, soaring midair in a twilight sky filled with violet auroras and floating petals.
2	A celestial lion with a translucent sapphire mane leaps through swirling galaxy clouds under a violet night sky, glowing stars trailing its paws.
3	A lone anthropomorphic fox in crystalline samurai armor, standing still in a bamboo grove made of glass, glowing runes etched into each plate.
4	A majestic griffin standing atop a wind-blown cliff at twilight, wings unfurled with feathers dripping golden light, oil-painting style.
5	A mystical fox-like humanoid with nine shimmering tails, guarding a floating paper lantern in a glowing sakura forest.
6	A half-human, half-clockwork artisan adjusting a glowing time orb inside a cathedral overgrown with vines.
7	A sculpture of a dog made entirely of reflective molten gold, mid-jump, fluid metallic texture, studio lighting.
8	A sci-fi poster with the bold title 'ASTRONOVA PRIME' in metallic lettering and lens flares.
9	A billboard on a desert highway showing 'Welcome to Dustvale', retro 70s font, sun flare.
10	A fairy marketplace hidden inside a giant blooming flower, stalls glowing with enchanted trinkets, fruit that floats midair.
11	A ruined celestial observatory at the edge of the world, cracked dome revealing a rotating sky-map of shifting stars.
12	A hyper-detailed dragon eye, glowing orange iris, reptilian skin.
13	A glamorous woman smiling in a glowing cosmic background.
14	A golden spellcircle inscribed with the phrase 'IGNIS SCRIPTUM' in liquid fire-gold runes, hovering midair.
15	A massive sand-carved monument showing 'CITY OF WHISPERS' in eroded stone calligraphy.
16	A magical contract floating in midair, the clause 'SOULBOUND BY NIGHTFALL' glowing in arcane script.
17	A medieval scroll displaying the phrase "Quest Accepted" in ornate gothic script.
18	A giant ancient coin partially buried in snow, engraved with 'DOMINION ETERNAL' around its rim.
19	A lizard monk painting 'Breathe, Don't Bite' in perfect cursive on rice paper with a brush.
20	A fox giving a TED talk titled 'Entropy and the Soul' written on a digital board behind.
21	A cat in a space suit skiing.
22	A small cactus with a happy face in the Sahara desert.
23	A dog jumping in front of moon gate, purple flowers, snowy mountains.
24	A Porsche 911 covered with leaves in a showroom.
25	A super cute Pikachu.
26	A man deadlifting heavy weights.
27	The rock Dwayne Johnson doing ballet.
28	Photorealistic fossilised bronze sculpture face portrait.
29	A magical deer made of stars standing at the edge of a glowing river under an aurora.
30	A knight made of ice stepping through a shattered stained-glass portal.
31	A cloaked traveler entering a glowing cavern of crystal pillars.
32	A mysterious violinist in a foggy alley playing notes that glow in the mist.
33	A royal skyship emerging from clouds at sunset, wings made of gold leaf and wind.
34	A fantasy tree sprouting glowing fruits under a swirling aurora sky.
35	A painting of a desert nomad holding a glowing hourglass, as time swirls around their robes.
36	Halloween scares up 918 min at global box office earns second highest horror opening of all time in North America.
37	SpaceX ready to send first all-civilian crew on orbit of Earth.
38	Waterfall surrounded by nice early summer flowers. Heather Foothills, Mt. Hood Meadows ski area, Oregon.
39	The One And Only by Tim Walker for Vogue May 2014.
40	HD Wallpaper.
41	Veiled Within.
42	Stevens.
43	Man stands near a waterfall.
44	A deer made of shimmering starlight grazing beside a silver river under a purple sky.
45	A crystal-winged butterfly landing on a dewdrop-covered spiderweb in a moonlit garden.
46	Milky way at the lake.
47	A phoenix rising from an ancient garden fountain, wings made of blooming petals and embers.
48	Fred Lyon - San Francisco   The Gallery at Leica Store San Francisco.
49	A graffiti mural on a city wall saying 'ART LIVES' in colorful spray-painted letters.
50	Newborn Baby Blanket Photography, Super Soft Photo, Basket Filler Basket Stuffer Prop.
51	A neon street sign that says 'CyberCore Café', glowing in magenta and blue.
52	An airship sail mid-tear in a storm, revealing the phrase 'WINDWRAITH CREST' half-blown away.
53	A magical sword embedded in stone, with the name 'SOLARFANG' etched along its blade.
54	A crow detective reading a paper titled 'Feathered Conspiracies', headline in bold gothic script.
55	A stop sign with 'ALL WAY' written below it.
56	A mechanical butterfly landing on a scroll that reads 'Silken Prophecy Delivered'.
57	An otter with a laser gun.
58	The bustling streets of Tokyo, crossroads, a beautiful girl in a sailor suit riding on the back of an Asian elephant.
59	8k resolution, realistic digital painting of a colossal dragon creature.
60	A dog swimming in space.
61	Whale Tail in water, award winning photo.
62	Inside a steampunk workshop, a young cute redhead inventor, wearing blue overalls and a glowing blue tattoo on her shoulder.
63	Kayak in the water, optical color, aerial view, rainbow.
64	A floating mountain temple where monks ride beams of light to meditate among the stars, surrounded by glowing lotus clouds.
65	A celestial stag made of lightning and auroras galloping across a stormy sky, leaving trails of stardust in its wake.

Table 15: Comprehensive list of prompts used across figures, experiments, and qualitative evaluations in the paper.

ID	Prompt
66	A sky harbor where airships dock on floating islands made of crystal, with rainbow waterfalls cascading into the clouds.
67	A glowing portal in the center of an ancient oak tree, guarded by moss-covered stone wolves under a violet twilight.
68	An underwater palace lit by jellyfish lanterns, where merfolk in ornate armor hold council in coral thrones.
69	A firefly festival deep in a bamboo forest, with floating lanterns and spirit masks glowing in warm twilight.
70	A dragon curled around a moonlit lighthouse, its scales reflecting stars while waves crash below in silver mist.
71	A library suspended in time, with floating books, glowing runes, and staircases that shift with every page turned.
72	A snowy village where aurora borealis is woven into tapestries by mythical weavers in glowing fur robes.
73	An enchanted canyon with floating stones engraved with prophecy, and golden birds nesting in the wind-carved cliffs.
74	A mermaid on a rocky shore, her tail shimmering with bioluminescent scales.
75	A warrior princess brandishing a crystal sword in the heart of a glowing battlefield.
76	A guardian golem carved from emerald stone standing vigil in ancient ruins.
77	A moonlit castle built atop a waterfall that glows with bioluminescent algae.
78	A floating island city above a sea of clouds with waterfalls cascading into the mist.
79	A twilight marketplace staffed by goblins selling glowing gemstones.
80	A colossal treebridge spanning two mountain peaks under the aurora borealis.
81	A sea of lavender with giant lotus flowers drifting toward a distant spired city.
82	A neon-lit dragonfly queen presiding over a phosphorescent swamp.
83	A crystal dragon coiled around an ancient tower under a tapestry of stars.
84	A marble statue of a goddess that comes to life at dawn's first light.
85	A hidden waterfall that pours rainbow mist into a crystal pool below.

649 **NeurIPS Paper Checklist**

650 The checklist is designed to encourage best practices for responsible machine learning research,  
651 addressing issues of reproducibility, transparency, research ethics, and societal impact. Do not remove  
652 the checklist: **The papers not including the checklist will be desk rejected.** The checklist should  
653 follow the references and follow the (optional) supplemental material. The checklist does NOT count  
654 towards the page limit.

655 Please read the checklist guidelines carefully for information on how to answer these questions. For  
656 each question in the checklist:

- 657 • You should answer [Yes] , [No] , or [NA] .
- 658 • [NA] means either that the question is Not Applicable for that particular paper or the  
659 relevant information is Not Available.
- 660 • Please provide a short (1–2 sentence) justification right after your answer (even for NA).

661 **The checklist answers are an integral part of your paper submission.** They are visible to the  
662 reviewers, area chairs, senior area chairs, and ethics reviewers. You will be asked to also include it  
663 (after eventual revisions) with the final version of your paper, and its final version will be published  
664 with the paper.

665 The reviewers of your paper will be asked to use the checklist as one of the factors in their evaluation.  
666 While "[Yes]" is generally preferable to "[No]", it is perfectly acceptable to answer "[No]" provided a  
667 proper justification is given (e.g., "error bars are not reported because it would be too computationally  
668 expensive" or "we were unable to find the license for the dataset we used"). In general, answering  
669 "[No]" or "[NA]" is not grounds for rejection. While the questions are phrased in a binary way, we  
670 acknowledge that the true answer is often more nuanced, so please just use your best judgment and  
671 write a justification to elaborate. All supporting evidence can appear either in the main paper or the  
672 supplemental material, provided in appendix. If you answer [Yes] to a question, in the justification  
673 please point to the section(s) where related material for the question can be found.

674 **IMPORTANT**, please:

- 675 • **Delete this instruction block, but keep the section heading “NeurIPS paper checklist”,**
- 676 • **Keep the checklist subsection headings, questions/answers and guidelines below.**
- 677 • **Do not modify the questions and only use the provided macros for your answers.**

678 **1. Claims**

679 Question: Do the main claims made in the abstract and introduction accurately reflect the  
680 paper's contributions and scope?

681 Answer: [Yes]

682 Justification: We have made main claims that accurately reflect the paper's contributions  
683 and scope in the abstract and the introduction.

684 Guidelines:

- 685 • The answer NA means that the abstract and introduction do not include the claims  
686 made in the paper.
- 687 • The abstract and/or introduction should clearly state the claims made, including the  
688 contributions made in the paper and important assumptions and limitations. A No or  
689 NA answer to this question will not be perceived well by the reviewers.
- 690 • The claims made should match theoretical and experimental results, and reflect how  
691 much the results can be expected to generalize to other settings.
- 692 • It is fine to include aspirational goals as motivation as long as it is clear that these goals  
693 are not attained by the paper.

694 **2. Limitations**

695 Question: Does the paper discuss the limitations of the work performed by the authors?

696 Answer: [Yes]

697 Justification: The paper discusses the limitations of this work.

698 Guidelines:

- 699 • The answer NA means that the paper has no limitation while the answer No means that  
700 the paper has limitations, but those are not discussed in the paper.
- 701 • The authors are encouraged to create a separate "Limitations" section in their paper.
- 702 • The paper should point out any strong assumptions and how robust the results are to  
703 violations of these assumptions (e.g., independence assumptions, noiseless settings,  
704 model well-specification, asymptotic approximations only holding locally). The authors  
705 should reflect on how these assumptions might be violated in practice and what the  
706 implications would be.
- 707 • The authors should reflect on the scope of the claims made, e.g., if the approach was  
708 only tested on a few datasets or with a few runs. In general, empirical results often  
709 depend on implicit assumptions, which should be articulated.
- 710 • The authors should reflect on the factors that influence the performance of the approach.  
711 For example, a facial recognition algorithm may perform poorly when image resolution  
712 is low or images are taken in low lighting. Or a speech-to-text system might not be  
713 used reliably to provide closed captions for online lectures because it fails to handle  
714 technical jargon.
- 715 • The authors should discuss the computational efficiency of the proposed algorithms  
716 and how they scale with dataset size.
- 717 • If applicable, the authors should discuss possible limitations of their approach to  
718 address problems of privacy and fairness.
- 719 • While the authors might fear that complete honesty about limitations might be used by  
720 reviewers as grounds for rejection, a worse outcome might be that reviewers discover  
721 limitations that aren't acknowledged in the paper. The authors should use their best  
722 judgment and recognize that individual actions in favor of transparency play an impor-  
723 tant role in developing norms that preserve the integrity of the community. Reviewers  
724 will be specifically instructed to not penalize honesty concerning limitations.

### 725 3. Theory Assumptions and Proofs

726 Question: For each theoretical result, does the paper provide the full set of assumptions and  
727 a complete (and correct) proof?

728 Answer: [Yes]

729 Justification: We provide the full set of assumptions in Section 3 and discuss the complete  
730 proof in detail in Appendix A.

731 Guidelines:

- 732 • The answer NA means that the paper does not include theoretical results.
- 733 • All the theorems, formulas, and proofs in the paper should be numbered and cross-  
734 referenced.
- 735 • All assumptions should be clearly stated or referenced in the statement of any theorems.
- 736 • The proofs can either appear in the main paper or the supplemental material, but if  
737 they appear in the supplemental material, the authors are encouraged to provide a short  
738 proof sketch to provide intuition.
- 739 • Inversely, any informal proof provided in the core of the paper should be complemented  
740 by formal proofs provided in appendix or supplemental material.
- 741 • Theorems and Lemmas that the proof relies upon should be properly referenced.

### 742 4. Experimental Result Reproducibility

743 Question: Does the paper fully disclose all the information needed to reproduce the main ex-  
744 perimental results of the paper to the extent that it affects the main claims and/or conclusions  
745 of the paper (regardless of whether the code and data are provided or not)?

746 Answer: [Yes]

747 Justification: The paper provides all the information needed to reproduce the main experi-  
748 mental results.

749 Guidelines:

- 750 • The answer NA means that the paper does not include experiments.
- 751 • If the paper includes experiments, a No answer to this question will not be perceived
- 752 well by the reviewers: Making the paper reproducible is important, regardless of
- 753 whether the code and data are provided or not.
- 754 • If the contribution is a dataset and/or model, the authors should describe the steps taken
- 755 to make their results reproducible or verifiable.
- 756 • Depending on the contribution, reproducibility can be accomplished in various ways.
- 757 For example, if the contribution is a novel architecture, describing the architecture fully
- 758 might suffice, or if the contribution is a specific model and empirical evaluation, it may
- 759 be necessary to either make it possible for others to replicate the model with the same
- 760 dataset, or provide access to the model. In general, releasing code and data is often
- 761 one good way to accomplish this, but reproducibility can also be provided via detailed
- 762 instructions for how to replicate the results, access to a hosted model (e.g., in the case
- 763 of a large language model), releasing of a model checkpoint, or other means that are
- 764 appropriate to the research performed.
- 765 • While NeurIPS does not require releasing code, the conference does require all submissions
- 766 to provide some reasonable avenue for reproducibility, which may depend on the
- 767 nature of the contribution. For example
- 768 (a) If the contribution is primarily a new algorithm, the paper should make it clear how
- 769 to reproduce that algorithm.
- 770 (b) If the contribution is primarily a new model architecture, the paper should describe
- 771 the architecture clearly and fully.
- 772 (c) If the contribution is a new model (e.g., a large language model), then there should
- 773 either be a way to access this model for reproducing the results or a way to reproduce
- 774 the model (e.g., with an open-source dataset or instructions for how to construct
- 775 the dataset).
- 776 (d) We recognize that reproducibility may be tricky in some cases, in which case
- 777 authors are welcome to describe the particular way they provide for reproducibility.
- 778 In the case of closed-source models, it may be that access to the model is limited in
- 779 some way (e.g., to registered users), but it should be possible for other researchers
- 780 to have some path to reproducing or verifying the results.

## 781 5. Open access to data and code

782 Question: Does the paper provide open access to the data and code, with sufficient instruc-

783 tions to faithfully reproduce the main experimental results, as described in supplemental

784 material?

785 Answer: [No]

786 Justification: We have provide the core file of our code in the supplementary. And the code

787 will be released upon acceptance.

788 Guidelines:

- 789 • The answer NA means that paper does not include experiments requiring code.
- 790 • Please see the NeurIPS code and data submission guidelines (<https://nips.cc/public/guides/CodeSubmissionPolicy>) for more details.
- 791 • While we encourage the release of code and data, we understand that this might not be
- 792 possible, so “No” is an acceptable answer. Papers cannot be rejected simply for not
- 793 including code, unless this is central to the contribution (e.g., for a new open-source
- 794 benchmark).
- 795 • The instructions should contain the exact command and environment needed to run to
- 796 reproduce the results. See the NeurIPS code and data submission guidelines (<https://nips.cc/public/guides/CodeSubmissionPolicy>) for more details.
- 797 • The authors should provide instructions on data access and preparation, including how
- 798 to access the raw data, preprocessed data, intermediate data, and generated data, etc.
- 799 • The authors should provide scripts to reproduce all experimental results for the new
- 800 proposed method and baselines. If only a subset of experiments are reproducible, they
- 801 should state which ones are omitted from the script and why.
- 802
- 803

- 804           • At submission time, to preserve anonymity, the authors should release anonymized  
805            versions (if applicable).  
806           • Providing as much information as possible in supplemental material (appended to the  
807            paper) is recommended, but including URLs to data and code is permitted.

808       **6. Experimental Setting/Details**

809       Question: Does the paper specify all the training and test details (e.g., data splits, hyper-  
810           parameters, how they were chosen, type of optimizer, etc.) necessary to understand the  
811           results?

812       Answer: [Yes]

813       Justification: The paper specify the all details of experiment, including hyper-parameters,  
814           the rationale for their selection and underlying model.

815       Guidelines:

- 816           • The answer NA means that the paper does not include experiments.  
817           • The experimental setting should be presented in the core of the paper to a level of detail  
818            that is necessary to appreciate the results and make sense of them.  
819           • The full details can be provided either with the code, in appendix, or as supplemental  
820            material.

821       **7. Experiment Statistical Significance**

822       Question: Does the paper report error bars suitably and correctly defined or other appropriate  
823           information about the statistical significance of the experiments?

824       Answer: [No]

825       Justification: We focused primarily on the exploratory analysis and preliminary results.  
826       Addressing statistical significance and error bars will be a priority in our future research to  
827           provide a more comprehensive evaluation of our findings.

828       Guidelines:

- 829           • The answer NA means that the paper does not include experiments.  
830           • The authors should answer "Yes" if the results are accompanied by error bars, confi-  
831            dence intervals, or statistical significance tests, at least for the experiments that support  
832            the main claims of the paper.  
833           • The factors of variability that the error bars are capturing should be clearly stated (for  
834            example, train/test split, initialization, random drawing of some parameter, or overall  
835            run with given experimental conditions).  
836           • The method for calculating the error bars should be explained (closed form formula,  
837            call to a library function, bootstrap, etc.)  
838           • The assumptions made should be given (e.g., Normally distributed errors).  
839           • It should be clear whether the error bar is the standard deviation or the standard error  
840            of the mean.  
841           • It is OK to report 1-sigma error bars, but one should state it. The authors should  
842            preferably report a 2-sigma error bar than state that they have a 96% CI, if the hypothesis  
843            of Normality of errors is not verified.  
844           • For asymmetric distributions, the authors should be careful not to show in tables or  
845            figures symmetric error bars that would yield results that are out of range (e.g. negative  
846            error rates).  
847           • If error bars are reported in tables or plots, The authors should explain in the text how  
848            they were calculated and reference the corresponding figures or tables in the text.

849       **8. Experiments Compute Resources**

850       Question: For each experiment, does the paper provide sufficient information on the com-  
851           puter resources (type of compute workers, memory, time of execution) needed to reproduce  
852           the experiments?

853       Answer: [Yes]

854       Justification: We provide implementation details including compute resource, time, etc.

855 Guidelines:

- The answer NA means that the paper does not include experiments.
- The paper should indicate the type of compute workers CPU or GPU, internal cluster, or cloud provider, including relevant memory and storage.
- The paper should provide the amount of compute required for each of the individual experimental runs as well as estimate the total compute.
- The paper should disclose whether the full research project required more compute than the experiments reported in the paper (e.g., preliminary or failed experiments that didn't make it into the paper).

864 **9. Code Of Ethics**

865 Question: Does the research conducted in the paper conform, in every respect, with the  
866 NeurIPS Code of Ethics <https://neurips.cc/public/EthicsGuidelines>?

867 Answer: [Yes]

868 Justification: The research conducted in the paper conform with the NeurIPS Code of Ethics  
869 in every respect.

870 Guidelines:

- The answer NA means that the authors have not reviewed the NeurIPS Code of Ethics.
- If the authors answer No, they should explain the special circumstances that require a deviation from the Code of Ethics.
- The authors should make sure to preserve anonymity (e.g., if there is a special consideration due to laws or regulations in their jurisdiction).

876 **10. Broader Impacts**

877 Question: Does the paper discuss both potential positive societal impacts and negative  
878 societal impacts of the work performed?

879 Answer: [Yes]

880 Justification: Yes, we discuss the broader impacts in appendix section G.

881 Guidelines:

- The answer NA means that there is no societal impact of the work performed.
- If the authors answer NA or No, they should explain why their work has no societal impact or why the paper does not address societal impact.
- Examples of negative societal impacts include potential malicious or unintended uses (e.g., disinformation, generating fake profiles, surveillance), fairness considerations (e.g., deployment of technologies that could make decisions that unfairly impact specific groups), privacy considerations, and security considerations.
- The conference expects that many papers will be foundational research and not tied to particular applications, let alone deployments. However, if there is a direct path to any negative applications, the authors should point it out. For example, it is legitimate to point out that an improvement in the quality of generative models could be used to generate deepfakes for disinformation. On the other hand, it is not needed to point out that a generic algorithm for optimizing neural networks could enable people to train models that generate Deepfakes faster.
- The authors should consider possible harms that could arise when the technology is being used as intended and functioning correctly, harms that could arise when the technology is being used as intended but gives incorrect results, and harms following from (intentional or unintentional) misuse of the technology.
- If there are negative societal impacts, the authors could also discuss possible mitigation strategies (e.g., gated release of models, providing defenses in addition to attacks, mechanisms for monitoring misuse, mechanisms to monitor how a system learns from feedback over time, improving the efficiency and accessibility of ML).

904 **11. Safeguards**

905 Question: Does the paper describe safeguards that have been put in place for responsible  
906 release of data or models that have a high risk for misuse (e.g., pretrained language models,  
907 image generators, or scraped datasets)?

908                  Answer: [Yes]

909                  Justification: Yes, we discuss it in section G in appendix.

910                  Guidelines:

- 911                  • The answer NA means that the paper poses no such risks.
- 912                  • Released models that have a high risk for misuse or dual-use should be released with  
913                  necessary safeguards to allow for controlled use of the model, for example by requiring  
914                  that users adhere to usage guidelines or restrictions to access the model or implementing  
915                  safety filters.
- 916                  • Datasets that have been scraped from the Internet could pose safety risks. The authors  
917                  should describe how they avoided releasing unsafe images.
- 918                  • We recognize that providing effective safeguards is challenging, and many papers do  
919                  not require this, but we encourage authors to take this into account and make a best  
920                  faith effort.

## 921                  12. Licenses for existing assets

922                  Question: Are the creators or original owners of assets (e.g., code, data, models), used in  
923                  the paper, properly credited and are the license and terms of use explicitly mentioned and  
924                  properly respected?

925                  Answer: [Yes]

926                  Justification: We follow the open-source codebases throughout our experiments, which are  
927                  credited properly.

928                  Guidelines:

- 929                  • The answer NA means that the paper does not use existing assets.
- 930                  • The authors should cite the original paper that produced the code package or dataset.
- 931                  • The authors should state which version of the asset is used and, if possible, include a  
932                  URL.
- 933                  • The name of the license (e.g., CC-BY 4.0) should be included for each asset.
- 934                  • For scraped data from a particular source (e.g., website), the copyright and terms of  
935                  service of that source should be provided.
- 936                  • If assets are released, the license, copyright information, and terms of use in the  
937                  package should be provided. For popular datasets, [paperswithcode.com/datasets](https://paperswithcode.com/datasets)  
938                  has curated licenses for some datasets. Their licensing guide can help determine the  
939                  license of a dataset.
- 940                  • For existing datasets that are re-packaged, both the original license and the license of  
941                  the derived asset (if it has changed) should be provided.
- 942                  • If this information is not available online, the authors are encouraged to reach out to  
943                  the asset's creators.

## 944                  13. New Assets

945                  Question: Are new assets introduced in the paper well documented and is the documentation  
946                  provided alongside the assets?

947                  Answer: [Yes]

948                  Justification: We provide demo code in supplementary material. The complete source code  
949                  will be released upon acceptance.

950                  Guidelines:

- 951                  • The answer NA means that the paper does not release new assets.
- 952                  • Researchers should communicate the details of the dataset/code/model as part of their  
953                  submissions via structured templates. This includes details about training, license,  
954                  limitations, etc.
- 955                  • The paper should discuss whether and how consent was obtained from people whose  
956                  asset is used.
- 957                  • At submission time, remember to anonymize your assets (if applicable). You can either  
958                  create an anonymized URL or include an anonymized zip file.

959       **14. Crowdsourcing and Research with Human Subjects**

960       Question: For crowdsourcing experiments and research with human subjects, does the paper  
961       include the full text of instructions given to participants and screenshots, if applicable, as  
962       well as details about compensation (if any)?

963       Answer: [Yes]

964       Justification: We discuss the details of subjective study briefly in main paper, and extensively  
965       in the appendix.

966       Guidelines:

- 967       • The answer NA means that the paper does not involve crowdsourcing nor research with  
968       human subjects.
- 969       • Including this information in the supplemental material is fine, but if the main contribu-  
970       tion of the paper involves human subjects, then as much detail as possible should be  
971       included in the main paper.
- 972       • According to the NeurIPS Code of Ethics, workers involved in data collection, curation,  
973       or other labor should be paid at least the minimum wage in the country of the data  
974       collector.

975       **15. Institutional Review Board (IRB) Approvals or Equivalent for Research with Human  
976       Subjects**

977       Question: Does the paper describe potential risks incurred by study participants, whether  
978       such risks were disclosed to the subjects, and whether Institutional Review Board (IRB)  
979       approvals (or an equivalent approval/review based on the requirements of your country or  
980       institution) were obtained?

981       Answer: [Yes]

982       Justification: Yes, IRB approvals were obtained for the subjective study. All participants  
983       have provided informed consent. All personal information was properly anonymized.

984       Guidelines:

- 985       • The answer NA means that the paper does not involve crowdsourcing nor research with  
986       human subjects.
- 987       • Depending on the country in which research is conducted, IRB approval (or equivalent)  
988       may be required for any human subjects research. If you obtained IRB approval, you  
989       should clearly state this in the paper.
- 990       • We recognize that the procedures for this may vary significantly between institutions  
991       and locations, and we expect authors to adhere to the NeurIPS Code of Ethics and the  
992       guidelines for their institution.
- 993       • For initial submissions, do not include any information that would break anonymity (if  
994       applicable), such as the institution conducting the review.